
An Investigation of the Endurance Limit of Hot-Mix Asphalt Concrete Using a New Uniaxial Fatigue Test Protocol



**University-Based Research, Education, and Technology Transfer Program
Contract NO. DTFH61-05-P-00159**

FINAL REPORT

May 31, 2006

By Ali Soltani, Mansour Solaimanian, David Anderson

PENNSTATE



Pennsylvania Transportation Institute

**The Pennsylvania State University
Transportation Research Building
University Park, PA 16802-4710
(814) 865-1891 www.pti.psu.edu**

1. Report No. FHWA-HIF-07-002		2. Government Accession No.		3. Recipient's Catalog No.	
4. Title and Subtitle An Investigation of the Endurance Limit of Hot-Mix Asphalt Concrete Using a New Uniaxial Fatigue Test Protocol				5. Report Date May 31, 2006	
				6. Performing Organization Code	
7. Author(s) Ali Soltani, Mansour Solaimanian, and David A. Anderson				8. Performing Organization Report No. 2006-17	
9. Performing Organization Name and Address The Pennsylvania Transportation Institute Transportation Research Building The Pennsylvania State University University Park, PA 16802-4710				10. Work Unit No. (TRAIS)	
				11. Contract or Grant No. DTFH61-05-P-00159	
12. Sponsoring Agency Name and Address Federal Highway Administration U.S. Department of Transportation Office of Acquisition Management 400 Seventh Street, SW Washington, DC 20590				13. Type of Report and Period Covered Final Report 6/16/2005 - 12/31/2005	
				14. Sponsoring Agency Code	
15. Supplementary Notes COTR: John D'Angelo, 202-366-0121					
16. Abstract: A research study was undertaken to investigate the existence of an endurance limit for hot-mix asphalt concrete using a new uniaxial fatigue testing protocol. The study included testing of four different mixtures. Cylindrical specimens, 120 mm in height and 80 mm in diameter, were tested by applying a tension-compression loading at 10 °C and 10 Hz. Each test included millions of cycles of sinusoidal loading with strain amplitudes of 20 and 30 μ -strain. The test results indicated that three of the mixtures tested exhibit an endurance limit below which no fatigue damage is expected regardless of the number of loading cycles applied. However, an endurance limit was not observed for one of the mixtures. This observation does not necessarily imply that for these mixtures such a limit does not exist, because some of the damage observed was the result of testing anomalies. Several problems with the data acquisition system as well as with the temperature control in the testing chamber caused interruptions in the testing. Although during the times that the test was being conducted excellent temperature and load control was exercised, some incremental improvements in the testing apparatus will be needed to remove the anomalies that were observed. A follow-on study is recommended during which the cause of the anomalies, their effect on the measured endurance limit, and means for their minimization would be studied. The improved procedure should then be extended to additional mixtures tested at different temperatures and strain levels.					
17. Key Words Fatigue, asphalt mixture, asphalt binder, uniaxial test, endurance limit				18. Distribution Statement No restrictions. This document is available from the National Technical Information Service, Springfield, VA 22161	
19. Security Classif. (of this report) Unclassified		20. Security Classif. (of this page) Unclassified		21. No. of Pages 57	22. Price

AN INVESTIGATION OF THE ENDURANCE LIMIT OF HOT MIX ASPHALT
CONCRETE USING A NEW UNIAXIAL FATIGUE TEST PROTOCOL

University-Based Research, Education, and Technology Transfer Program
Contract No. DTFH61-05-P-00159

FINAL REPORT

Prepared for

Federal Highway Administration
U.S. Department of Transportation

By
Ali Soltani
Mansour Solaimanian
and
David A. Anderson

The Pennsylvania Transportation Institute
The Pennsylvania State University
Transportation Research Building
University Park, PA 16802-4710

May 31, 2006

PTI 2006-17

This work was sponsored by the U.S. Department of Transportation, Federal Highway Administration. The contents of this report reflect the views of the authors, who are responsible for the facts and the accuracy of the data presented herein. The contents do not necessarily reflect the official views or policies of the Federal Highway Administration, U.S. Department of Transportation. This report does not constitute a standard, specification, or regulation.

Acknowledgments

This project was funded by Federal Highway Administration contract FHWA DTFH61-05-P-00159. The support of Mr. John D'Angelo of the Federal Highway Administration is greatly appreciated. Mr. Darin Hunter is also acknowledged for assistance provided in the laboratory.

Table of Contents

Introduction.....	1
Objectives	1
Literature Review.....	1
Research Plan.....	2
Test Equipment.....	3
Data Acquisition System and Testing Machine.....	3
Temperature Measurements.....	4
Data Synchronization.....	4
Environmental Chamber.....	7
Test Fixtures and Specimen Mounting.....	7
Materials and Specimen Preparation	9
Properties of Mixtures.....	10
Fatigue Testing.....	10
Experimental Results	12
Temperature Control.....	12
Fatigue Response	14
Parameters Derived from Protocol Testing.....	16
Discussion, Comments, and Findings.....	17
Conclusions.....	21
Recommendations.....	22
References.....	23
Appendix A: Properties of Tested Specimens	A-1
Appendix B: Graphs Presenting Fatigue Testing Results.....	B-1

List of Figures

Figure 1. Photograph of test fixtures, specimen, transducers and thermocouples	2
Figure 2. Location of thermocouples on the test specimen.	5
Figure 3. Example of the effect of data synchronization on variability in the measured modulus	6
Figure 4. Schematic of temperature chamber and controller	7
Figure 5. Schematic of test fixture.....	8
Figure 6. Schematic of loading in Stages I, II, and III.....	11
Figure 7. Testing at specific strain levels to validate existence of the endurance limit..	11
Figure 8. Air temperature in the environmental chamber during M32987 testing.	13
Figure 9. M21673 specimen surface temperature at location TC2.....	13
Figure 10. Schematic demonstrating drift phenomenon.....	19
Figure 11. Drift during the test for specimen 21673.....	20
Figure 12. Drift during the test for specimen 21676.....	21

List of Tables

Table 1. Data acquisition schedule for each stage.....	4
Table 2. Properties of the mixtures prepared for this research.	9
Table 3. Problems encountered during testing.....	14
Table 4. Specimens tested and the corresponding schedule.....	15
Table 5. Summary of results from the fatigue tests conducted in this research.....	17
Table 6. The change in modulus from Stage I to Stage III for different specimens.....	20

Introduction

Fatigue cracking is one of the major distresses in hot-mix asphalt (HMA) concrete pavements, and a fatigue distressed pavement is very costly to repair. Fatigue cracking can originate from the bottom of the pavement layer propagating to the top, or it can originate from the pavement surface propagating to the bottom. The magnitude and frequency of loads, environmental conditions, engineering properties of the hot-mix asphalt concrete, condition of underlying layers, and pavement structure are all contributing factors to fatigue cracking.

A major controlling factor for bottom-up fatigue cracking is the magnitude of the tensile strain at the bottom of the HMA layer. It is a well-established concept in pavement design that decreasing this tensile strain results in an increase in pavement fatigue life. It is also believed by some asphalt and pavement design experts that an endurance limit exists for HMA. If the tensile strain is maintained at levels below the endurance limit, the pavement will have infinite fatigue life. National Cooperative Highway Research Project NCHRP 9-38 is an ongoing study investigating the validity of the endurance limit hypothesis and the effect of HMA materials, mixture factors and testing conditions on the endurance limit.

Objectives

The research study presented in this report was conducted to investigate existence of an endurance limit for a limited number of hot-mix asphalt mixtures under uniaxial sinusoidal tension-compression loading.

Literature Review

The presence of an endurance limit is a well-recognized behavior for ferrous materials such as steel. However, limited research has been conducted for HMA and the existence of an endurance limit, and factors affecting it, if it does exist, are not well known at this point. The possible existence of an endurance limit for hot-mix asphalt concrete (HMAC) has been ignored by most researchers studying the fatigue behavior of asphalt mixtures in the laboratory. However, as pointed out by Carpenter et al., in 1970 Monismith et al. suggested that an endurance limit exists for HMAC and suggested 70 μ -strain as a likely value (1). Carpenter et al. recently addressed the question of the existence of an endurance limit in HMAC, concluding that an endurance limit does exist and that it is in the range of 70 to 90 μ -strain at 20 °C for a loading frequency of 10 Hz (2). Based on a damage analysis of laboratory test results obtained from a uniaxial tension-compression test, Soltani postulated the presence of an endurance limit for two mixtures tested at 10 °C and 10 Hz. He estimated endurance limits of 30 and 80 μ -strains for the two mixtures that contained unmodified binder and modified binder, respectively (3).

Research Plan

The testing configuration and protocol used in this study to establish the presence of an endurance limit for asphalt mixtures is very similar to that used previously for FHWA/PennDOT-sponsored fatigue research (4). Major deviations from the previous study are in the preparation of test specimens, some improvements in the control, data acquisition and analysis software, and the use of a more appropriate load cell with smaller capacity. For the research presented here, cylindrical test specimens were cored and saw cut from Superpave Gyrotory Compactor specimens. A photograph of the test specimen, fixtures, transducers and thermocouples is shown in Figure 1.

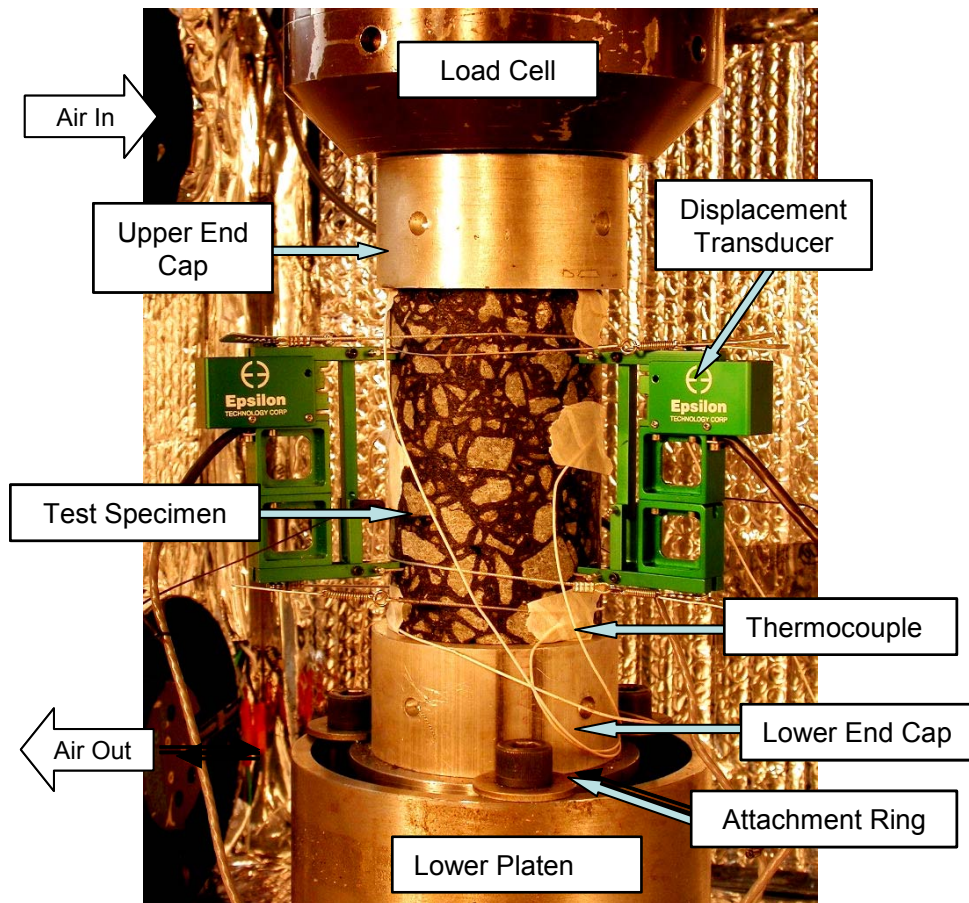


Figure 1. Photograph of test fixtures, specimen, transducers and thermocouples.

The testing was conducted in the controlled strain (displacement) mode using cylindrical test specimens. In this type of loading the state of stress and strain inside the middle portion of the test specimen can be considered uniform, as long as the specimen is homogeneous, the ends of the specimen are restrained from rotation, and the applied load is concentric with the axis of the test specimen. The following test conditions were selected for this study:

- Test loading: sinusoidal centered at zero (push-pull configuration);
- Test frequency: 10 Hz;
- Test temperature: 10 °C;
- Strain: 20 to 30 μ -strain;
- Specimen: cylindrical, 75.5-mm diameter by 120-mm height;
- Gauge length: 75 mm; and
- Test mode: constant strain (controlled displacement by one transducer).

Test Equipment

Details of the test equipment are reported elsewhere (4). Details regarding the testing equipment and data acquisition relevant to this study are presented below.

Data Acquisition System and Testing Machine

The electronics included an Instron Model 8800 System equipped with FastTrack™ software and hardware. The FastTrack™ 8800 unit, which contains two general purpose interface bus (GPIB) boards each with four channels of data acquisition, is used to control the servo valve that controls the pressure in the hydraulic actuator. The first GPIB board communicates with the position, load, strain 1, and strain 2 channels. The second GPIB board communicates with the strain 3 channel.

The FastTrack™ 8800 unit, which is itself a computer, receives commands from either a hardware source or from another computer that generates commands through software. Instron provides a separate Man-Machine Interface (MMI) that can be used as a hardware source. The Instron multi-axial library (which is appropriate when more than one GPIB board is in use) was used in developing the LabVIEW™ data acquisition and control program for this study.

Specimen displacement was measured with three Epsilon transducers that were interfaced with the FastTrack™ 8800 hardware. Data were collected from the actuator LVDT, the load cell and each of the three displacement transducers at the rate of 100 points/cycle/channel (1 KHz/channel). Data were collected and analyzed using LabVIEW™. Excel™ files of reduced data were generated by LabVIEW™ for plotting and further analysis. The approach presented by Chapra and Canale (5) was used to apply sinusoidal signal curve fitting to the data obtained from all channels. The curve fitting was used to generate the stress and strain amplitude and phase angle data.

An MTS 5-KN load cell was used in this study to measure the load magnitude. This lower-capacity load cell was utilized to improve the resolution in measuring the load since very low load levels were needed to induce the targeted strain levels. This is a change from the previous study (4) where a 100-kN load cell was utilized.

The rate of data logging was adjusted in concordance with the rate of change in the modulus or to the importance of the loading cycles. Consequently, at the beginning of

each stage when the modulus is either dropping (Stages I and II) or recovering (Stage III) the data for the first 100 cycles and the last 100 cycles of the stage were acquired. For other cycles of each stage, the cycles used for data collection can be found in Table 1.

Table 1. Data acquisition schedule for each stage.

Range in Cycles	Number of Cycles between Measurements
First 100 cycles of Stage	1
Cycles 101 to 1,000 of Stage	20
Cycles 1,001 to 1,000 of Stage	100
Cycles 1,001 to 100 cycles prior to end of Stage	1,000
Last 100 Cycles of Stage	1

Temperature Measurements

Eighteen thermocouples (TC) were used for the measurement of temperature at various points. The specimen surface temperature was measured using nine thermocouples (Figure 2). One TC was placed in the middle of each pair of transducer contact points (thermocouples 2, 5, and 8). Above and below each transducer, three thermocouples were placed at the very top of the specimen (thermocouples 1, 4, and 7), and three thermocouples were placed at the very bottom of the specimen (thermocouples 3, 6, and 9). TC 10 was placed in the water bath and TC 11 was placed next to the RTD that controls the test chamber temperature. Thermocouples 12 and 13 were placed on the upper and lower aluminum heads and TC 14 was placed on the load cell. The air temperature of the walk-in chamber was monitored with the built-in thermocouple of the multiplexer. TC 15 was placed at the mid center of a dummy specimen and TC 16 at its center. The laboratory ambient air temperature was monitored with the built-in thermocouple of the Micrologger.

An AM25T multiplexer and a Campbell Scientific CR23x Micrologger were used to collect and store temperature data. Temperature measurements were obtained once per minute during the fatigue testing and synchronized in the time domain with the dynamic measurements obtained with the FastTrack™ software.

Data Synchronization

The complexity of the data acquisition system requires caution with respect to the synchronization of the data. If the computer in the Fast Track 8800 cannot acquire and process data fast enough to prevent buffer overruns, data from the various channels will not be properly synchronized in time. The results of this problem can be seen as excessive variability in the plots of modulus versus loading cycles as shown in Figure 3.

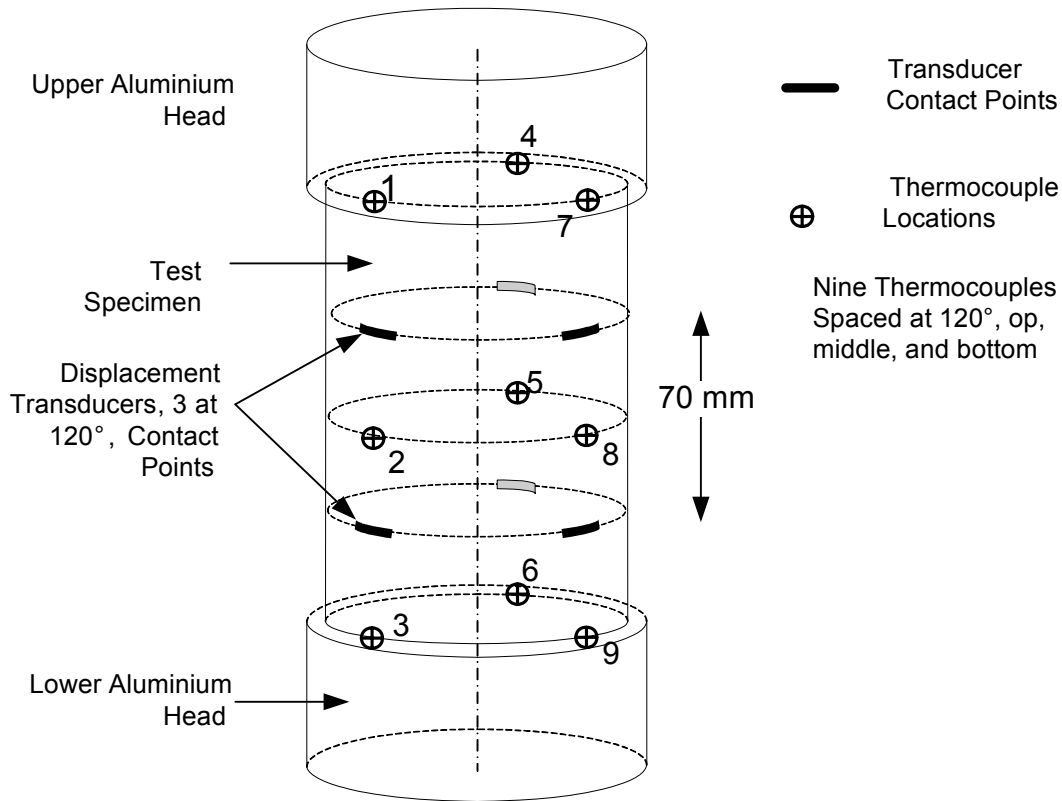


Figure 2. Location of thermocouples on the test specimen.

As discussed above, the data are collected from two separate GPIB boards (number 3 and 4) within the Fast Track 8800. Except for transducer 3 all the channels are located on GPIB 3. The Fast Track 8800 system is in charge of keeping GPIB 3 and 4 synchronized so all the collected data are obtained at the same time. Data synchronization is well maintained by Fast Track 8800 as long as the buffer is not full. If for any reason the computer does not read the data fast enough from the buffer, the buffer becomes full and Fast Track 8800 loses its ability to keep the two GPIB boards synchronized. If such an event occurs, data from GPIB 4 (where transducer 3 is connected) are no longer synchronized with GPIB 3 (where the rest of channels are connected). Unfortunately from the moment Fast Track 8800 loses its ability to maintain synchronization, all the collected data are desynchronized, even after the buffer is fully read and empty.

In normal situations the speed of reading the data by the Fast Track 8800 computer is sufficient to prevent buffer overruns. This keeps the buffer empty almost all the time, ensuring that no data are lost by overwriting. In the event that the computer processor is busy with some other tasks, then there is a risk that the buffer will overflow. To avoid this situation all the possible actions were taken to be certain that the computer was fully and exclusively devoted to the task of data acquisition. All possible services were turned off; the computer was disconnected from the network, the antivirus was disabled, all the services from the operating system were deactivated, and temperature data acquisition

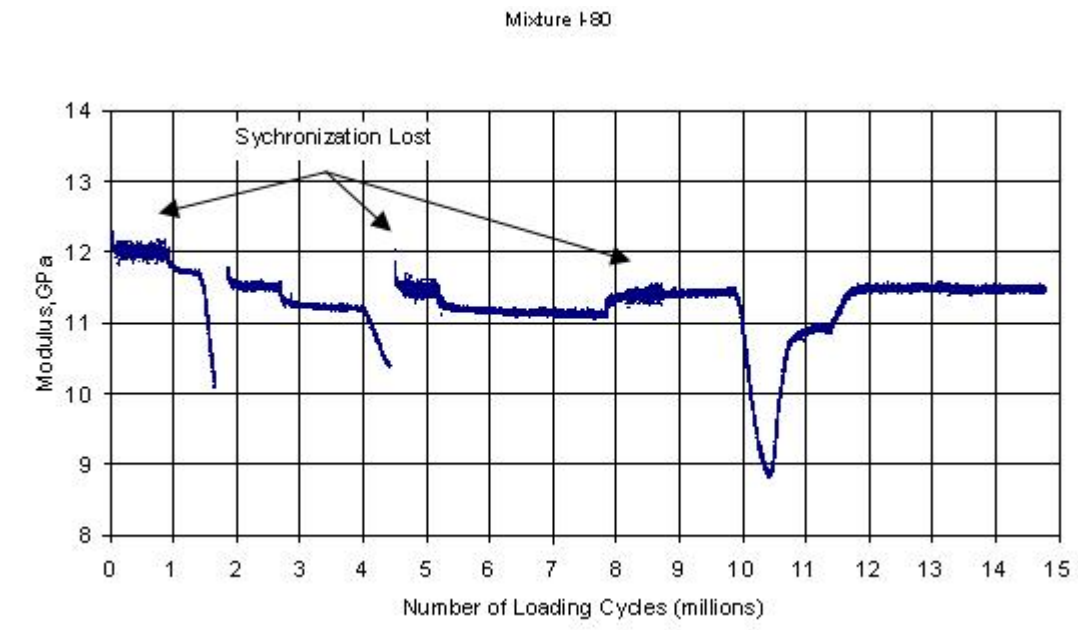


Figure 3. Example of the effect of data synchronization on variability in the measured modulus.

was loaded on a separate computer. Although these actions reduced the number of times that this problem occurred, only at the end of this project was it realized that some unknown application(s) was (were) occasionally taking processor time and causing the data not to be synchronized.

At the beginning of the project, when the data synchronization problem was first realized, the only solution immediately available was to stop and restart the loading when the buffer overflow occurred. This could add some other risks to the testing in addition to the fact that any discontinuity in the loading applied to the specimen affected its modulus. As a consequence a new module was programmed and added to the control and data acquisition software. This module allowed the operator to reset the buffer and to synchronize the data without any interruption in the loading. The only downside of this procedure was that it was not automatic and required that the operator be continuously present during the test and intervene manually. This meant that from the moment the problem occurred until the moment the operator noticed the problem and reset the buffer, the collected data were not synchronized.

During the testing in this project the difference in time between the first appearance of unsynchronized data collected from transducer 3 and the two others was limited to a maximum of 2 seconds (or 20 cycles). During those time periods in the testing where the variation of modulus was very small, the effect of unsynchronized data on the analysis was negligible. This is especially true for the calculation of the slope of modulus at the end of the stages where there were a large number of data points.

For future testing either a system upgrade will be needed to solve this problem or a module must be added to the control and data acquisition system to periodically check

whether the data are synchronized or not. The added module will automatically reset the buffer in the event that the data are not synchronized.

Environmental Chamber

A dual chamber scheme was used to control the testing temperature (Figure 4). The test chamber was mounted inside a walk-in environmental chamber. The temperature inside the test chamber was controlled by connecting a water bath to a heat exchanger mounted in a plenum adjacent to the test chamber. Air was exchanged between the plenum and the test chamber resulting in variations of less than ± 0.015 °C in the test chamber. Two 100-W light bulbs were used as a heat source to make small adjustments in the temperature of the air passing between the plenum and the test chamber.

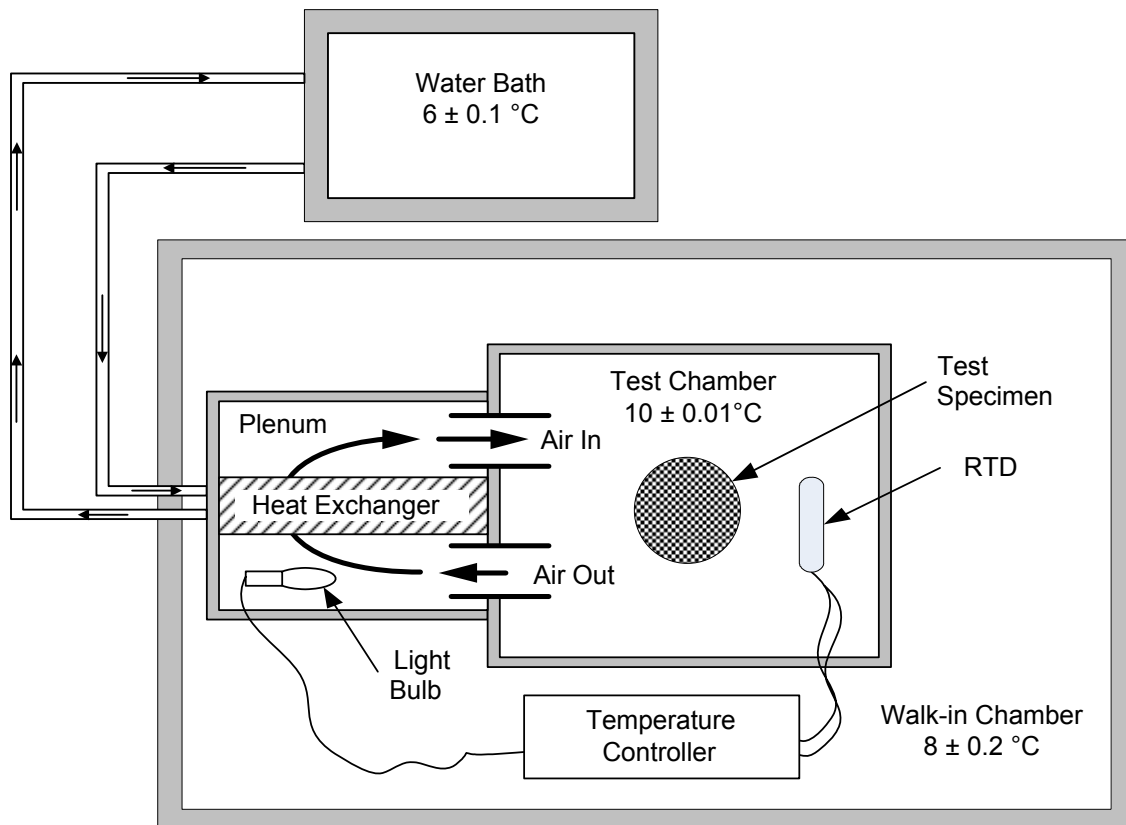


Figure 4. Schematic of temperature chamber and controller.

Test Fixtures and Specimen Mounting

A schematic of the test fixture including a test specimen and the transducers is given in Figure 5. A jig was used to align the mounting heads and test specimen during the gluing process. The jig ensures that the ends of the mounting heads as they are attached to the testing frame are parallel and that the axes of the test specimen and mounting heads are concentric.

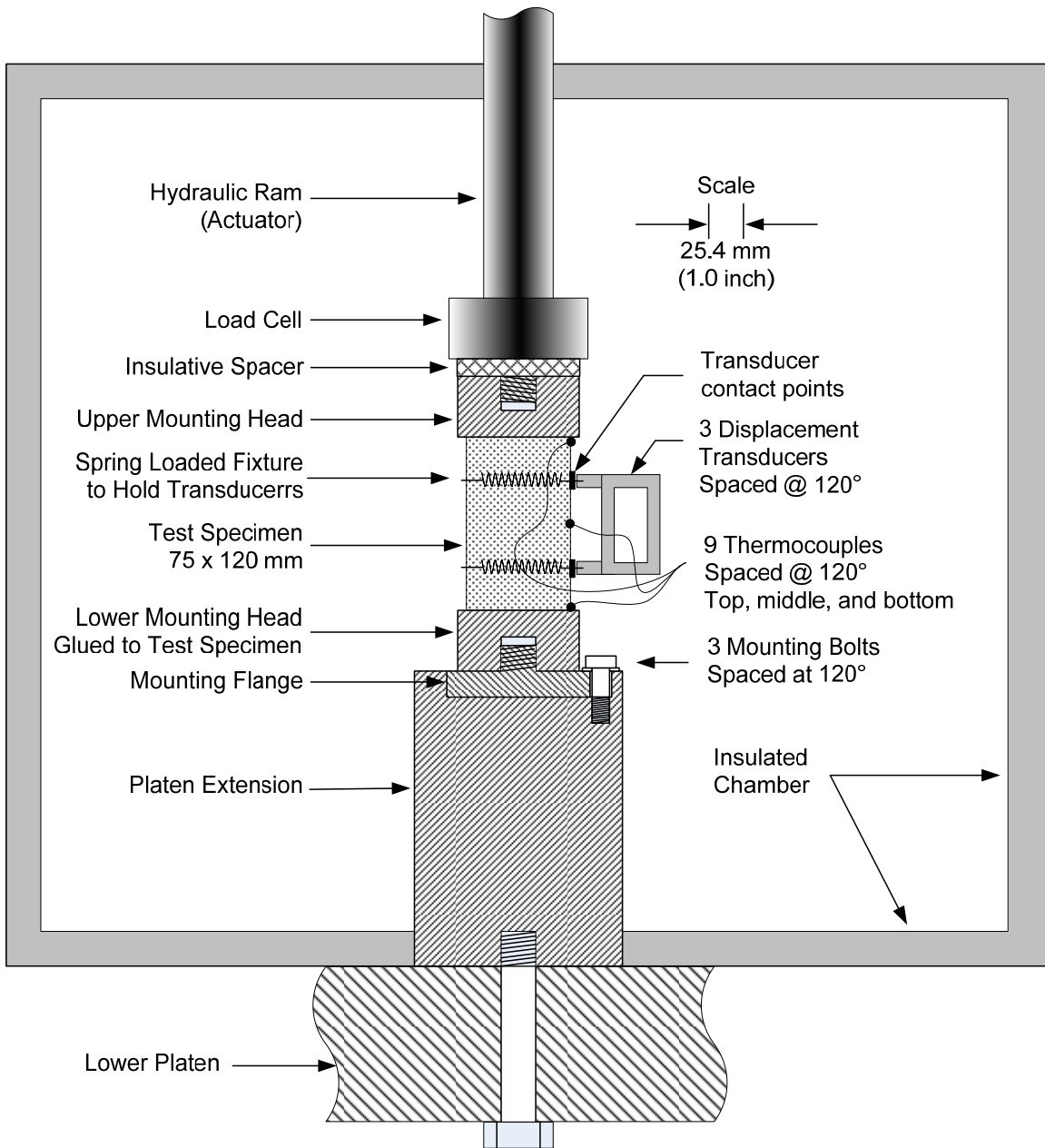


Figure 5. Schematic of test fixture.

In order to prepare a specimen for testing, the test specimen is placed in the jig along with the epoxy-coated upper and lower mounting heads. After the epoxy has cured, the specimens are maintained in the temperature chamber for 24 hours at the test temperature for conditioning and achieving temperature equilibrium. The lower mounting head and the mounting flange are screwed together, and then the upper mounting head is screwed into the load cell. The hydraulic ram is lowered until the mounting flange seats on the lower platen extension. The three bolts connecting the mounting flange and the lower platen extension are then tightened. With this configuration, the ends of the test specimen

are held rigidly in the testing machine. By following this procedure damage to the test specimen caused by traction, compression or torque is minimized.

Materials and Specimen Preparation

The original experiment design included four different asphalt mixtures with three replicates for each. However, because a number of problems were incurred during the course of the project, changes were made to the original experiment design. Table 2 presents the mixtures and specimens prepared for this study.

Table 2. Properties of the mixtures prepared for this research.

Mix ID	PG Grade	Target AV%	Specimen #	Actual AV%	%AC
M1241A	PG 64-22	7.0	5	6.8	4.9
			6	7.4	
			7	7.9	
M2167	PG 76-22	7.0	3	7.0	4.7
			5	6.8	
			6	6.7	
			7	6.8	
			8	6.2	
M3298	PG 64-22	7.0	1	7.4	5.5
			2	7.3	
			5	6.2	
			6	7.3	
			7	6.4	
M5201	PG 58-28	7.0	9	6.8	5.0
			10	6.5	
			11	6.6	
I-80	PG 76-22	7.0	-----	6.6	5.3

With the exception of the I-80 specimen the specimens were compacted using a Pine™ Superpave Gyrotory Compactor. The compacted specimens were 150 mm in diameter and 150 mm in height. Attempts were made to achieve air voids in the range of 7.0 ± 0.5

percent. The I-80 specimens were compacted as part of a previous fatigue study using the French rolling wheel compactor as described elsewhere (4).

Properties of Mixtures

The gradation and properties for the mixtures prepared for this study are presented in Appendix A. Three of the mixes were obtained from a PennDOT-sponsored project, Superpave In-Situ Stress-Strain Investigation (SISSI).

The I-80 mix was used in the previous fatigue study (4). Unfortunately, due to time constraints no tests were conducted on the last mix (M5201) and limited testing was conducted on the remaining mixes.

Fatigue Testing

During a previous study (6), a new fatigue testing protocol was proposed in which three stages of continuous loading without any rest period were considered, as shown in Figure 6. Schematic of loading in Stages I, II, and III. The same strain level, not exceeding the endurance limit of the HMA and consequently at a level that does not produce fatigue damage, is applied during Stages I and III. During Stage II, a strain with a magnitude exceeding the endurance limit and consequently causing fatigue damage is applied. The difference between the moduli at the end of Stages I and III (represented by two asymptotes) should directly indicate the level of “true” fatigue damage imposed during Stage II, as shown in Figure 6. Schematic of loading in Stages I, II, and III.

Damage should occur during Stage II only if the strain level during Stage II is greater than the endurance limit. In the study presented here, strain levels were expected to be considerably less than if the endurance limit were applied. For both Stages I and III, strain magnitude is maintained at the same level (ϵ_1). For Stage II, a larger strain level ϵ_2 is applied. At each stage, loading continues until the curve of modulus versus number of cycles reaches a zero slope (i.e., $S_{AB} = S_{CD} = S_{FG} = 0$, where S indicates the slope of line presenting modulus as a function of loading cycles). The expectation is that the modulus at the end of Stage III will return to the same level as was observed at the end of Stage I if the applied strains are below the endurance limit. Therefore, the following goals will be achieved from such an experiment:

1. Demonstrate that the drop in modulus during Stage II is not the result of fatigue damage. This is believed to be the case when at the end of Stage III the modulus returns to the original level E_1 of Stage I once strain is reduced from ϵ_2 to ϵ_1 (as shown in Figure 7).
2. Demonstrate that the induced strains ϵ_I and ϵ_{II} are indeed within the endurance limit, even though a drop in modulus is observed during Stages I and II; and
3. Verify the existence of an endurance limit for the mixtures that is equal to or greater than ϵ_2 .

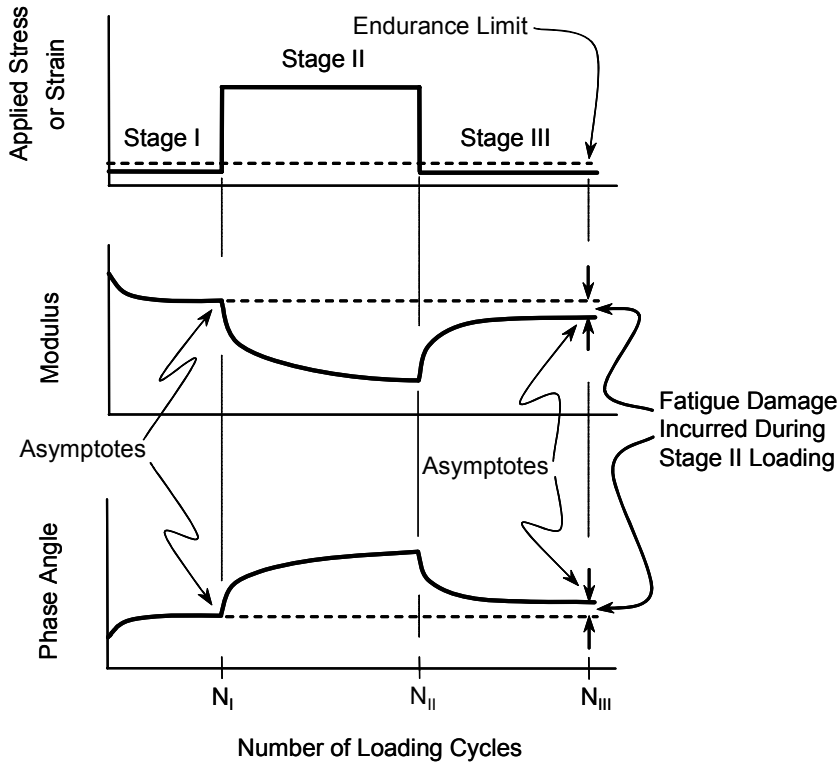


Figure 6. Schematic of loading in Stages I, II, and III.

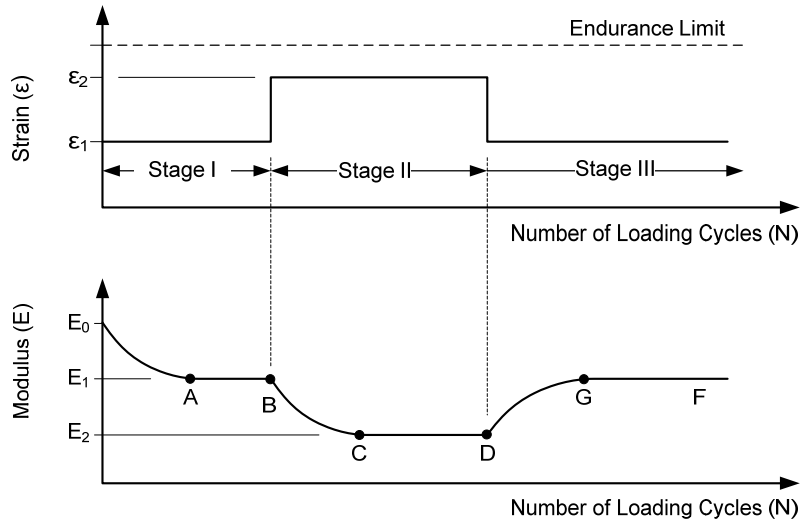


Figure 7. Testing at specific strain levels to validate existence of the endurance limit.

Experimental Results

Temperature Control

An important aspect of HMA testing in general is the control of the temperature, since at ambient temperatures a variation of 1 °C typically results in a 6 percent variation in the HMA modulus. The control of temperature during HMA testing for determination of endurance limit becomes particularly important since very small variations of modulus are investigated to establish the asymptote. If temperature is not well controlled the variation of modulus caused by temperature variations will mask or overwhelm the effect of fatigue or recovery.

In this study the temperature of the specimen was very well controlled as shown by Figure 8, which shows data obtained from the temperature of air in the test chamber during the testing of specimen M32987. The standard deviation in the temperature is 0.0243 °C. With the improvements made during this study to the temperature control and data acquisition system, the amount of self heating at very low strain was directly measured at the specimen surface. One example of such a measurement, accomplished for the first time on HMA for the very small strains used in this study, is shown in Figure 9. In this figure part of the test between cycles 2,000,000 and 3,000,000 containing Stages I and II for Specimen M21673 is presented. Specimen surface temperature data in this figure were obtained from TC 2, located on the surface of the test specimen midway between the contact points for the control transducer, Figure 2. As can be seen in Figure 9, the increase of strain amplitude from 20 to 30 μ -strain generates about 0.01 °C self-heating at the specimen surface, approximately a 0.05 percent in modulus. This temperature change has minimal effect on the modulus.

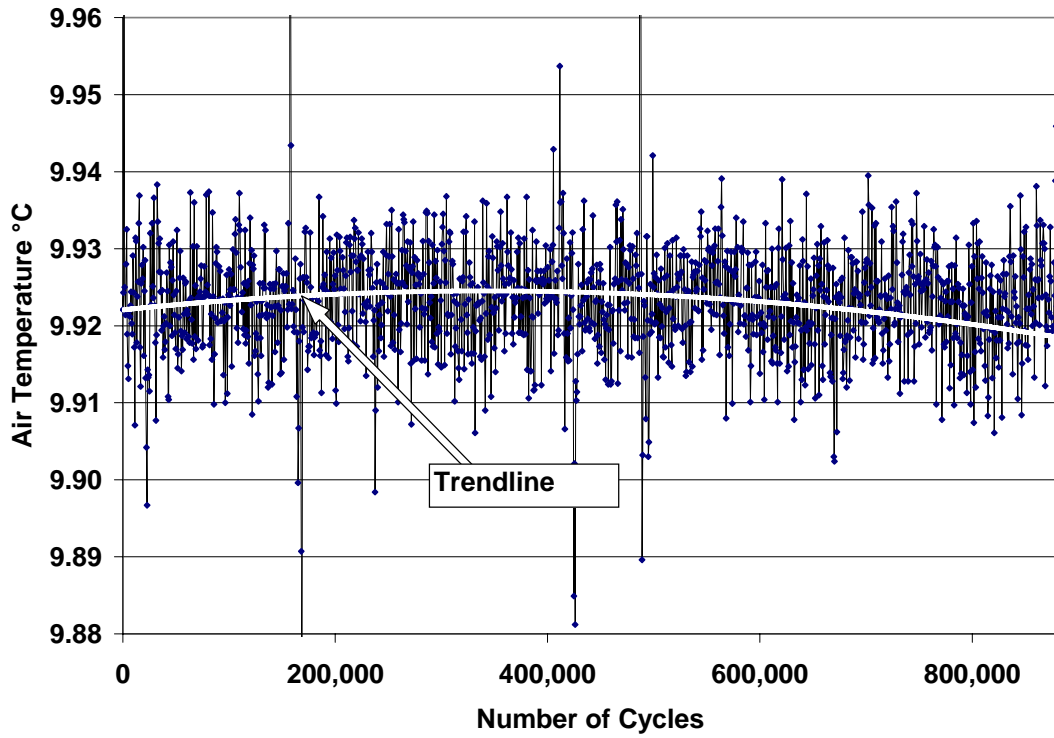


Figure 8. Air temperature in the environmental chamber during M32987 testing.

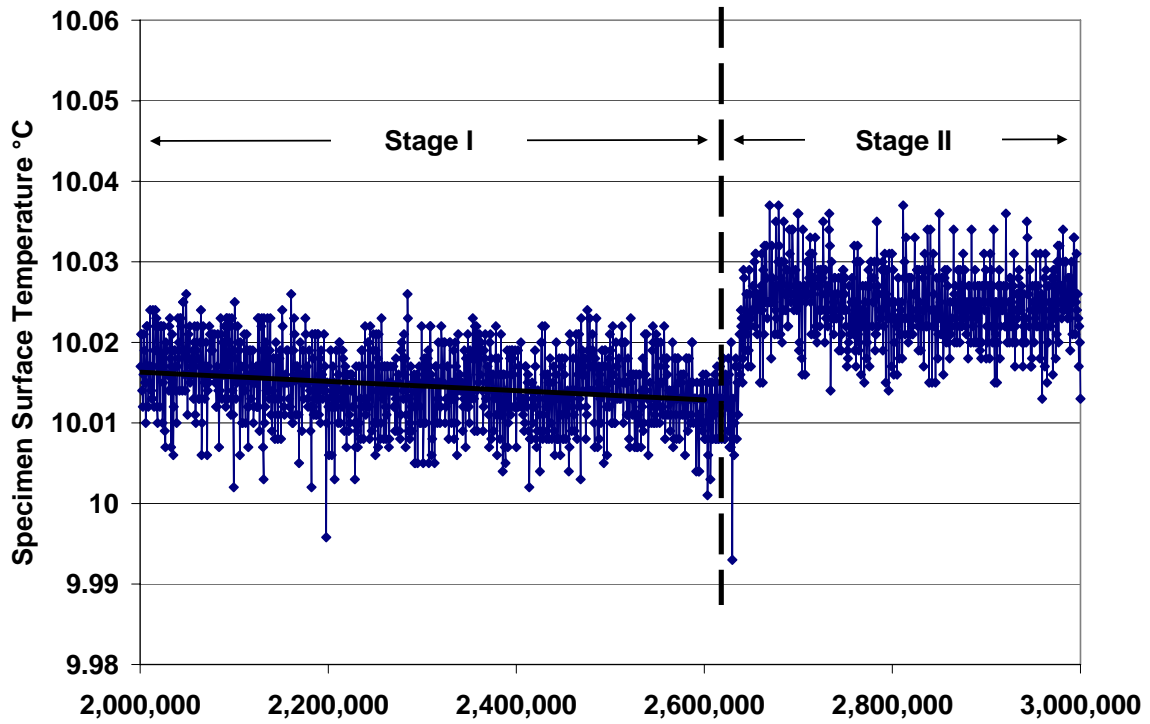


Figure 9. M21673 specimen surface temperature at location TC2.

Fatigue Response

The results presented here were generated from millions of cycles of loading. Unfortunately, due to the impact of several problems (primarily external to the testing itself), continuity in the test conditions could not be fully maintained throughout the period of testing. A list of the various problems that were encountered during the testing is given in Table 3. Specific events occurred at different times to either halt the testing or to change the test conditions. Once such an event occurred, proper action took place to either resume the test or to bring the testing conditions back to normal. Each label is subsequently followed by an explanation of the event and the action taken to resolve the issue.

In each test, the objective was to generate a continuous testing condition for the three stages needed to verify the existence of an endurance limit. As a result, if the impact of an interfering event was considerable, a new three-stage testing sequence was imposed on the specimen after corrective action was taken. The results of this study on the endurance limit can be valid only if continuity in the loading was maintained during the three successive stages of the fatigue protocol. This is because the HMA recovers its modulus immediately after any interruption in the loading. If the loading is interrupted, the testing must be re-started for Stage I, only after giving a few hours of rest time to the specimen. This ensures that the difference between the moduli at the end of Stages I and III is not related to any self-healing as a result of loading interruption.

Table 3. Problems encountered during testing.

Problem	Solution
A. Fast Track 8800 GPIB board ceased to function.	Purchased new board.
B. Computer motherboard ceased to function.	Purchased new board.
C. Hydraulic power shut down because of Master frame interference caused by running two machines simultaneously.	Coordinated with other researchers to prevent testing simultaneously on different machines using the same hydraulic power supply. Adjustments to the software system were needed to allow other tests to be conducted simultaneously with the fatigue test.
D. Temperature in walk-in chamber out of control.	Repaired twice and finally a new compressor was purchased and installed.
E. Unscheduled loss of electrical power.	Rebooted the system and restarted the loading (return to start of Stage I).
F. Loading synchronization disabled.	Partial loss of data.
G. Fast Track 8800 would not reset after rebooting.	New clock chipsets were purchased and installed on each of the 4 GPIB boards.

Because this project was of short duration (four months of actual activity period) and with limited resources it was decided to maximize the results by fully allocating the four

months of the project to the laboratory testing. A total of six specimens were tested during the course of this project. Table 4 shows the testing schedule for the tested specimens. The first five weeks of the project were spent on the specimen fabrication, installation and calibration of a new load cell, making new fixtures for the attachment of the new load cell, programming software for data analysis, adaptation of the existent software to the loading of the new fatigue protocol, a new program for temperature data collection, improvements in the insulation of the testing chamber, installation of temperature acquisition devices and thermocouples, running dummy testing and adjustment of new PID settings for the loading control. During this time the data acquisition board of the Fast Track 8800 ceased to function and was replaced by a new one. The experimental part of the research was organized so that during each testing sequence the next specimen would have been prepared and conditioned at the desire temperature. This allowed the testing to be run nearly continuously with almost no lost testing time. While the research was in progress many changes and improvements were made to the control and data acquisition and analysis software, especially to address the problems external to the testing itself, Table 4 presents the tested specimens and the corresponding testing schedule.

Table 4. Specimens tested and the corresponding schedule.

Specimen ID	Start Date	Start Time	Completion Date	Completion Time	Remarks
M21677	10/10/2005				After installation and before loading, due to hydraulic problems, specimen broke.
M21676	10/11/2005	8:02	10/25/2005	8:12	Several interfering events delayed testing.
I80-60	10/26/2005	11:01	11/15/2005	10:47	
M21673	11/17/2005	18:08	12/6/2005	16:37	
M32987	12/6/2005 12/7/2005	17:37 9:26	12/6/2005 12/8/2005	9:54	Specimen broke at the top at the beginning of the test. Only load control compression test was applied.
M32986	12/8/2005	16:43	12/31/2005	16:34	
M12415	1/2/2006	14:37	1/6/2006	14:00	Tested only at 30 microstrain for all cycles.

As shown in the preceding table, of the seven specimens subject to testing, for only four specimens (i.e. M21676, I-80, M21673, and M32986) could the conditions of the proposed protocol be met. Table 4 also indicates that for some of the specimens testing took considerable time to complete. This was partly because a test has to be restarted when a loading interruption occurs and partly because of some extra testing that was added for further study of material behavior. For example, the start and completion dates for specimen M32986 are 12/8/2005 and 12/31/2005, respectively, indicating a testing period of 23 days. The first two weeks of this period included two attempts to conduct the fatigue protocol. The remaining period dealt with various tests on the specimen to investigate the impact of various factors on the results as discussed later. This period also included frequency sweep testing and final breaking of the specimen.

The loading history and the reduced data for the entire loading sequence for each of the four specimens are presented in Appendix B as a series of graphs. A summary of the results is presented in Table 5. All of the tests were conducted at 10 °C and 10 Hz. Each attempt at applying the test protocol represents the application of three successive stages until the completion of Stage III, where a definite asymptote is reached. When for any reason this sequence was not obtained, another test was attempted after allowing the specimen to rest for a few hours. If the operator observed that an asymptote was not reached in Stage II, Stage III could be initiated without additional waiting (rest). Similarly the operator could stop the test if Stage III did not show the possibility that the specimens would fully recover. This was in particular the case of specimen M21673, which failed to reach an asymptote during low strain level, indicating the absence of an endurance limit. However, the loading history of this specimen prior to the application of the protocol loading is suspect with the likelihood that it was damaged before the testing was started. Only three of the test specimens (I-80, M32986, and M21696) were loaded in a manner that could be used to test for the existence of an endurance limit.

Parameters Derived from Protocol Testing

The various parameters reported in Table 5 were used to verify the presence of an endurance limit. E_o (not to be confused with initial modulus) and E_n are the specimen moduli at cycle N_o and N_n , respectively. Both are obtained based on a linear regression on the modulus data between cycles N_o and N_n . Cycles N_o and N_n are arbitrarily chosen at the end of any given stage in order to estimate the slope of modulus versus number of cycles.

ΔN represents the total number of cycles on which the slope of the regressed line was obtained. It is equal to the difference between E_n and E_o . Slope, expressed as a percentage, represents the slope of regressed line after being normalized by the value of E_o . Slope is given in terms of the percentage of variation of normalized modulus per million cycles, on the order of 10^{-8} per cycle. Its sign is negative (positive) for decreasing (increasing) values of modulus versus number of cycles. This is an extremely small rate of change and may for practical purposes be considered as a zero slope.

Period of calculation indicates the stage for which N_o and N_n were chosen. The number of cycles given under the heading “1st cycle of the test” indicates the total number of cycles that the specimen has sustained in the previous attempts at applying the protocol.

Reaching a line with a slope equal to exactly zero (a horizontal asymptote) is practically impossible when it comes to the variation of modulus versus number of cycles. In this research the criterion chosen to conclude that such a line was reached was the point at which the absolute value of the normalized slope of the regressed line at the end of Stage I and II was less than 0.2×10^{-8} GPa per cycle. Although this value was chosen arbitrarily, its choice can be justified because it is exceedingly small and would be of no consequence in terms of pavement life. Further, the calculated values for the slope were often negative, indicating that the small values reported for the slope may be the result of experimental error rather than material behavior.

Table 5. Summary of results from the fatigue tests conducted in this research.

Specimen	Test Sequence	Eo MPa	En MPa	No	Nn	NN (Nn-No)	Slope %/million cycle	Period of calculation	1st cycle of the attempted test
M32986	First Attempt	11,909 11,628	11,889 11,606	877,000 2,894,000	1,821,310 3,170,000	944,310 276,000	-0.175 -0.687	End of Stage I End of Stage II	1
	Second Attempt	11,947 11,539 11,773	11,942 11,526 11,778	3,625,000 7,465,000 10,124,000	4,099,919 8,309,937 10,847,010	474,919 844,937 723,010	-0.082 -0.129 0.056	End of Stage I End of Stage II End of Stage III	3,200,000
M21673	First Attempt	14,672	14,659	399,000	2,637,700	2,238,700	-0.038	End of Stage I	1
		14,045	13,959	7,155,000	7,952,000	797,000	-0.769	End of Stage II	
		14,162	14,171	9,968,000	10,484,170	516,170	0.134	End of Stage III	
I-80	First Attempt	12,008	12,007	241,000	822,000	581,000	-0.014	End of Stage I	1
		11,716	11,699	1,251,000	1,363,000	112,000	-1.342	End of Stage II	
	Second Attempt	11,516 11,212	11,516 11,203	2,111,000 3,628,050	2,654,000 3,953,050	543,000 325,000	-0.007 -0.255	End of Stage I End of Stage II	1,850,000
M21676	Third Attempt	11,480	11,480	4,704,000	5,171,906	467,906	-0.003	End of Stage I	4,490,000
		11,128	11,126	7,122,000	7,787,000	665,000	-0.028	End of Stage II	
		11,473	11,473	13,686,000	14,764,000	1,078,000	-0.003	End of Stage III	
M21676	First Attempt	14,593 14,425	14,584 14,414	2,845,000 4,158,000	3,539,008 4,523,000	694,008 365,000	-0.087 -0.200	End of Stage I End of Stage II	1
	Second Attempt	14683 14452 14544	14672 14443 14558	4789000 8367000 10812000	6113906 10369938 11372000	1324906 2002938 560000	-0.055 -0.030 0.169	End of Stage I End of Stage II End of Stage III	4,523,000

Discussion, Comments, and Findings

The primary focus of this work was to verify the existence of an endurance limit for HMAC under uniaxial cyclic compression-tension fatigue testing. Under the conditions of the test procedure used for this research, the primary criterion in deciding whether such a limit exists is the difference between the magnitude of modulus at the end of Stage I and at the end of Stage III. In the case that there is no difference, it can be concluded that the maximum strain applied to the specimen (30 μ -strain for this study) does not exceed the endurance limit and indeed such a limit exists. If there is a difference between the magnitude of modulus from the end of Stage I compared with the end of Stage III, it could be concluded that fatigue damage has occurred and the applied strain exceeds the endurance limit, or that artifacts in the test procedure have caused the loss in modulus. It should be pointed out that the stress levels are very low and the test duration is very long, such that small testing artifacts can potentially lead to significant effects on the results.

The graphs detailing variation of modulus, phase angle, and temperature as functions of loading cycles are presented in Appendix B. In the tests conducted in this research, the slope of the line defining modulus as a function of number of cycles was the criterion used to decide when the strain level should be changed from Stage I to Stage II (i.e., from 20 μ -strain to 30 μ -strain) or from Stage II to Stage III (i.e., from 30 μ -strain to 20 μ -strain). Ideally, this slope should approach zero before the stage is changed. The line used for determining this slope was the regression line for the last several hundred

thousand loading cycles of each stage. As shown in Table 5, for those cases in which the testing proceeded to Stage III, for all specimens, the slope was less than 0.2 percent per million cycles of loading (i.e., every million cycles of loading causes a 0.2 percent drop in modulus).

The major question to answer, in case there is a drop of modulus from the end of Stage I to the end of Stage III, is whether an acceptable limit could be adopted for this drop in modulus to allow the confirmation of an endurance limit. Indeed, due to many contributing factors, it would be logical to expect small changes in the modulus without concluding that such a change is the result of fatigue damage. Table 6 provides a summary of results for modulus and the percent drop for each specimen at the end of Stages I and III for the last cycle of loading. It could safely be concluded that specimens I-80 and M21676 have not exhibited any damage. However, the response for specimens M32986 and M21673 is questionable in this regard. M21673 and M21676 are replicate specimens from the same mix, showing very different behaviors in terms of damage. A closer investigation of the results indicates that specimen M21673 has been exposed to expansive drift during the test while specimen M21676 has tolerated a compressive drift (Figures 9 and 10, respectively). This conclusion is evident from the strain values plotted for each of these two specimens.

The drift that occurred in the displacement measurements for the two transducers that were not in the control loop is of concern. Little information can be found in the literature regarding this effect, its cause, and its effect on the modulus or fatigue behavior. The researchers concluded that further investigation is required into the cause of this effect and its influence on the interpretation of the test results before continuing with the validation of the proposed fatigue protocol. The test results presented in this report are based on controlled strain conditions; that is, one of the displacement transducers was included in the testing machine control loop. The drift issue can be best explained by reference to Figure 10, where L_o represents the initial gauge length for the control transducer. The baseline gauge length of this transducer remains constant because it is in the control loop. The “drift,” as it is referred to in this report, is the change in the baseline gauge length of the two transducers that are not in the control loop. (Note that the oscillatory strain is superimposed on the baseline gauge length. The baseline represents the center of the amplitude of the sinusoidal strain.)

The drift recorded for test specimens M21673 and M21676 is shown in Figures 11 and 12, respectively. The drift in the baseline gauge length for the strain 2 and strain 3 transducers is on the order of tens of microns, whereas the amplitude of the strain is approximately 2 microns. If the gauge length between the transducers were to change uniformly by 75 microns (μm), the axial strain would be 1000 μ -strain (i.e., one tenth of a percent), exceedingly large in comparison to the 20-30 μ -strain which is the peak-to-peak strain amplitude applied as part of the protocol. To gain a further insight as to the relevance of the baseline drift, if the specimen undergoes 1000 μ -strain in the axial direction without any change in lateral dimension, the change in volume would be one tenth of a percent, slightly affecting the modulus. If lateral dimension change is considered, assuming a Poisson’s ratio of 0.2, the change in volume would be approximately 0.06 percent, resulting in an even smaller impact on modulus. The change

in modulus caused by such a volume change (due to drift) will not be very important for cases when the modulus is used for pavement design purposes. However, for endurance limit fatigue tests, where very slight variations in modulus should be investigated for establishing the endurance limit, such volume changes may become important. Therefore, the cause and effect of the baseline drift needs to be investigated with the objective of identifying its cause and minimizing it to the extent that the test results are not affected. Although it was beyond the scope of this project to research the baseline drift, a number of reasons for this drift can be postulated. These include rotation of the ends of the specimen caused by insufficient rigidity of the system, which would cause the specimen to “bend.” Even assuming that the ends of the specimen do not rotate, there is the possibility that the internal displacements within the test specimen are not symmetric with respect to the axis of the specimen, thereby causing it to distort.

A number of sources for rotation and distortion can be postulated; lateral deflection of the actuator and the rotational stiffness of the load cell or other fixture components exacerbated by inhomogeneity of the specimen (i.e., modulus), differences in the tensile and compressive moduli, and eccentricity of the applied load. These and other effects need to be evaluated in a follow-on study before any additional fatigue testing is performed. The behavior of the specimen should also be investigated when measuring the specimen deformation from the top platen to the bottom platen at the same time measurements are conducted within the 75 mm gauge length. This measurement technique will help to investigate how deformation is taking place within the specimen.

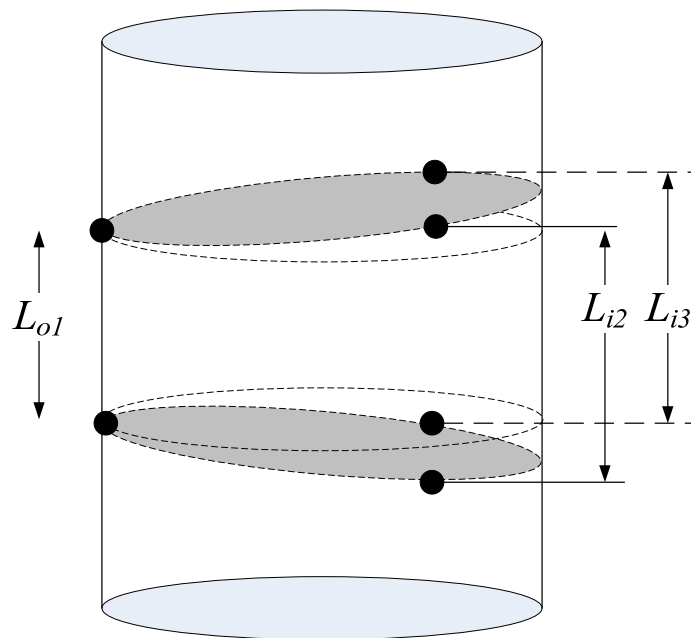


Figure 10. Schematic demonstrating drift phenomenon.

Table 6. The change in modulus from Stage I to Stage III for different specimens.

Specimen	E_{n-I} , MPa	E_{n-III} , MPa	Drop in E , %
M32986	11,942	11778	1.37
M21673	14,659	14171	3.33
I-80	11,480	11473	0.06
M21676	14672	14558	0.78

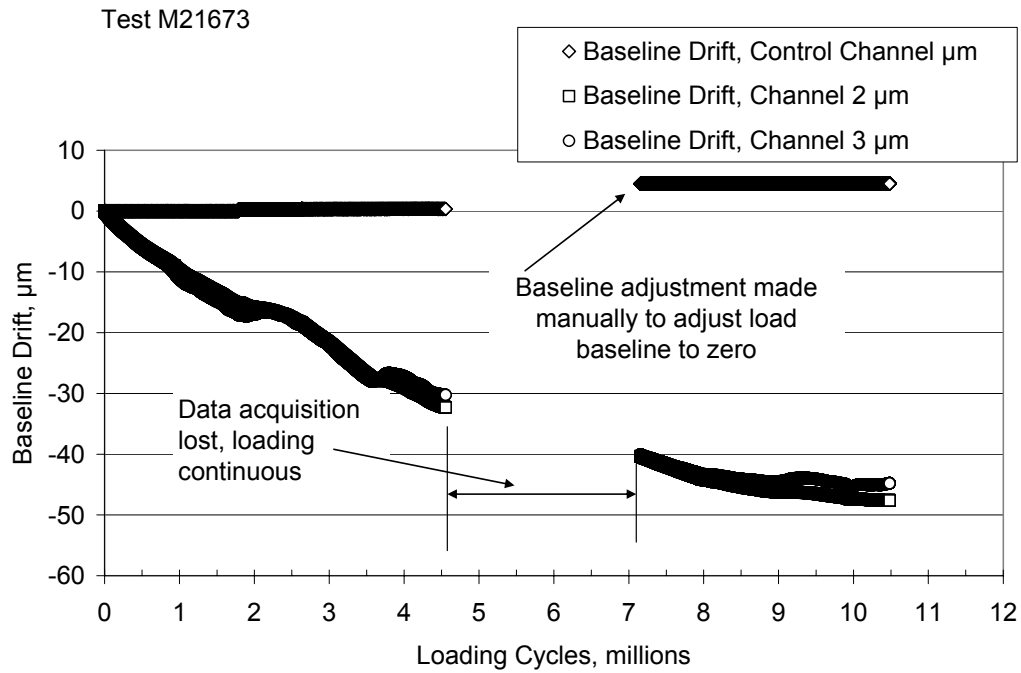


Figure 11. Drift during the test for specimen 21673.

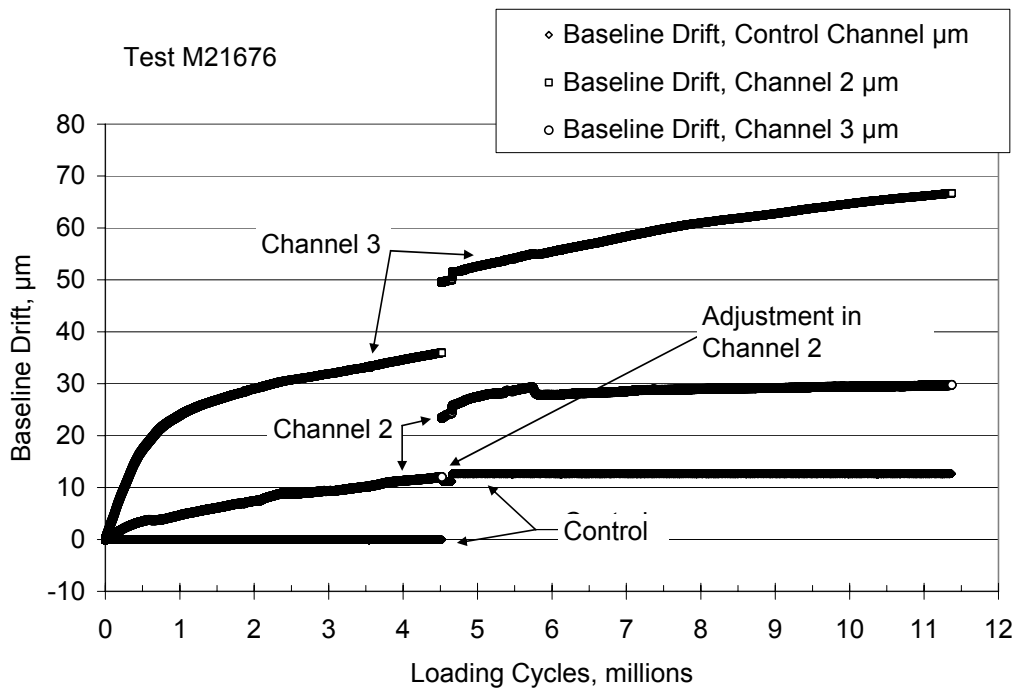


Figure 12. Drift during the test for specimen 21676.

Conclusions

Based on the work conducted during this study and the materials and testing protocols that were used, the following conclusions are drawn:

- Under the testing procedure followed during this research some specimens have shown no fatigue damage after millions of cycles of loading when subjected to strain amplitudes of 30 μ -strain. These results suggest that an endurance limit exists for at least some mixtures and that the endurance limit is at least 30 μ -strain at 10 °C and under the other testing conditions used for the study.
- One of the test specimens showed significant damage as a result of the testing protocol followed during this study, while the others did not. From this it can be concluded that if all HMAC mixtures possess an endurance limit, testing anomalies caused load-induced damage during the loading of this specimen. Alternatively it can be concluded that either the endurance limit for the specimen in question is less than 30 μ -strain, or not all HMAC mixtures exhibit an endurance limit.
- Anomalies in the test data suggest that the test as performed may be less homogeneous than assumed. Of particular concern is the baseline drift observed in the uncontrolled displacement transducers. From this it can be concluded that additional effort is needed to refine the test procedure and to identify and eliminate as best possible the anomalous behavior.

- The results of this study provide strong evidence for the presence of an endurance limit for HMAC. However, the results are not conclusive because the effect of testing anomalies is not known. Consequently, a review of the testing conditions is needed to identify and correct the source of anomalous behavior.

Recommendations

Based on the results of this study the authors recommend that the research be continued, with two short-term objectives.

- First, before any additional fatigue testing is conducted, the testing configuration need should be reviewed in detail to minimize the anomalous behavior that was observed during this study. Of particular concern is the nonuniformity in the displacement measurements as evidenced by the sometimes large drift in the baseline readings as experienced by the two displacement transducers that were not in the feedback loop. Items that need to be investigated include eccentricity in the applied load, homogeneity of the modulus across the test specimen, the rotational and axial compliance of the testing machine and its fixtures and the protocol used to mount the test specimen among other items that have not yet been identified. Both analytical and laboratory testing will be required to accomplish this task.
- The main objective of a follow-on study should be to continue the effort required to validate the presence of an endurance limit using the specimens that were not tested during this study. This would include replicate test specimens to provide information on the repeatability of the test results. The study should be extended to include the mixtures that were not tested during this study, ideally to include some of the mixtures being evaluated as part of the NCHRP 9-38 Project. The testing must also include provision for replicate measurements at different strain levels.
- Future studies should expand the protocol to larger Stage II strains and to testing conducted in load control and in compression-only and tension-only modes.
- Investigating fatigue behavior and the existence of an endurance limit requires lengthy and extensive testing for each specimen. Unfortunately, because of equipment problems encountered in the course of testing as well as the extended time required for testing each individual specimen, it was not possible to conduct the tests on all of the specimens prepared for this study. It is recommended that the tests be conducted on the remaining prepared specimens so that conclusive evidence could be provided for an endurance limit.

A detailed work plan for a follow-on study is presented in Appendix A. The work plan includes a key detailed review of the test apparatus and the testing of mixtures that were not tested during this study to include replicate measurements.

References

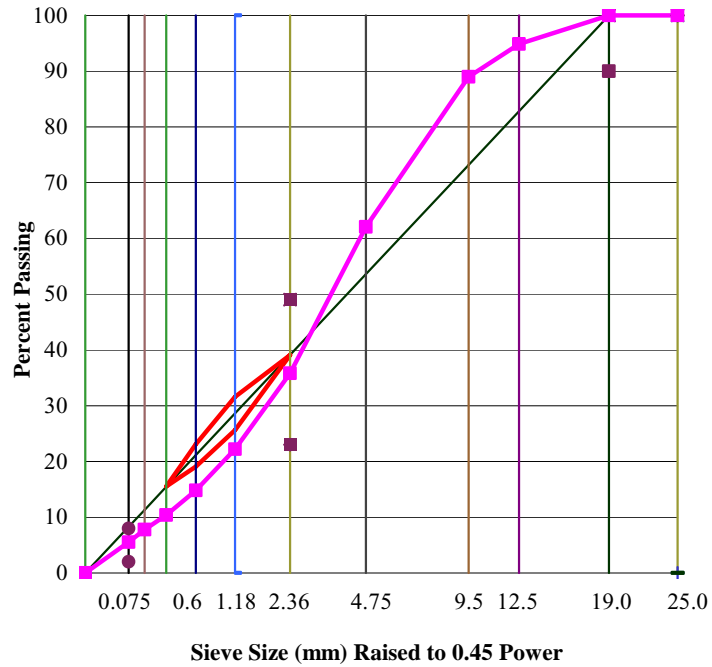
1. Monismith, C. L., J. A. Epps, D. A. Kasianchunk, and D. B. McLean, *Asphalt Mixture Behavior in Repeated Flexure*, Report No. TE 70-5, Institute of Transportation and Traffic Engineering, University of California, Berkeley, 1970.
2. Carpenter, S. H., K. A. Ghuzlan, and S. Shen, "A Fatigue Endurance Limit for Highway and Airport Pavements." Paper No. 03-3428, presented at the Annual Meeting of the Transportation Research Board, January 2003.
3. Soltani, A., "Comportement en Fatigue des Enrobes Bitumineux," Doctoral Dissertation, Ecole Nationale des Travaux Publics de l'Etat - INSA, Lyon, France, 1998.
4. Soltani, A., and D. A. Anderson, *Uniaxial Fatigue of Asphalt Mixes: A New Approach*, Report No. PTI 2003-13, Pennsylvania Transportation Institute, The Pennsylvania State University, January 2005.
5. Chapra, S.C., and R.P. Canale, *Numerical Methods for Engineers*, McGraw-Hill, New York, 1988, Section 13.1.
6. Soltani, A., and D. A. Anderson, "New Test Protocol to Measure Fatigue Damage in Asphalt Mixtures," *Journal of Road Materials and Pavement Design*, Vol. 4, 2005.

APPENDIX A

PROPERTIES OF TESTED SPECIMENS

Summary of Mix Design Information
Mix Type: 12.5-mm (ID M3298)

Sieves	SI,mm	%Pass
Units	Units	Combnd
1	25	100.0
3/4	19	100.0
1/2	12.5	94.9
3/8	9.5	89.0
#4	4.75	62.1
#8	2.36	35.8
#16	1.18	22.2
#30	0.6	14.8
#50	0.3	10.4
#100	0.15	7.8
#200	0.075	5.5
pan	0	0.0



Percentages of Different Aggregates			
A67(E)	A8(E)	A8	B3
11.3	11.3	22.4	55.0

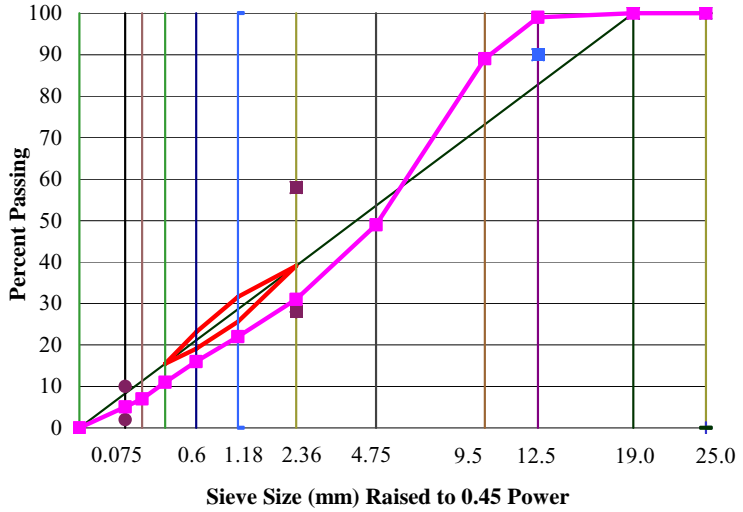
Aggregate Nominal Max Size	12.5 mm
Binder Grade and Source	PG 64-22
Binder Source	Marathon

$N_{des.}$	100	$N_{initial}$	8	N_{max}	160
G_b (Binder Specific Gravity)		1.028		P_b (% Binder Content)	5.5
G_{sb} (Agg. Bulk Sp. Gr.)		2.745		P_{ba} (absorbed as % mass of agg)	0.4
G_{se} (Aggr. Effective Sp. Gr.)		2.771		P_{be} (effective as % of total mix)	5.2
G_{mb} (Mix Bulk Sp. Gr.)		2.350		% Pass 0.075-mm Sieve	5.5
				G_{mm} (Mix Max. Theor. Sp. Gr.)	2.535

%AV	7.3	%VMA	19.1
% G_{mm}	92.7	%VFA	61.8
		D/AC	1.07

Summary of Mix Design Information
Mix Type: 12.5-mm (ID M2167)

Sieves	SI,mm	%Pass
US	Units	Combnd
1	25	100.0
3/4	19	100.0
1/2	12.5	99.0
3/8	9.5	89.0
#4	4.75	49.0
#8	2.36	31.0
#16	1.18	22.0
#30	0.6	16.0
#50	0.3	11.0
#100	0.15	7.0
#200	0.075	5.1
pan	0	0.0



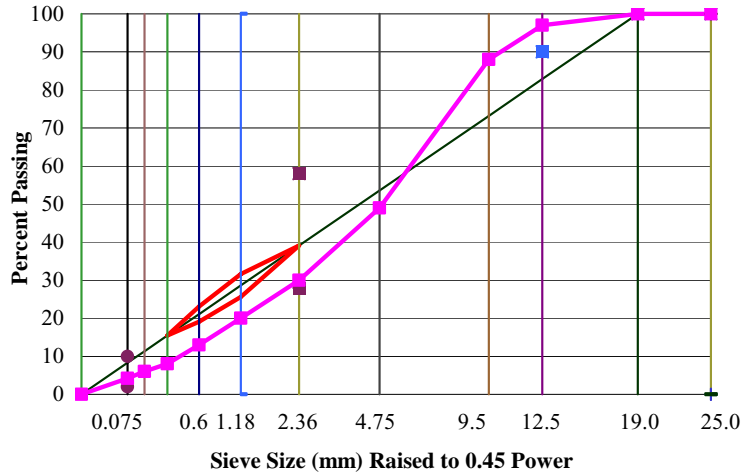
Percentages of Different Aggregates					Aggregate Nominal Max Size 12.5 mm
207B1	B-1	#8	#7	RAP	Binder Grade PG 76-22
6.6	11.2	51.8	14.8	15.6	

$N_{des.}$	100	$N_{initial}$	8	N_{max}	160
G_b (Binder Specific Gravity)		1.037		P_b (% Binder Content)	4.7
G_{sb} (Agg. Bulk Sp. Gr.)		2.602		P_{ba} (absorbed as % mass of agg)	0.5
G_{se} (Aggr. Effective Sp. Gr.)		2.635		P_{be} (effective as % of total mix)	4.2
G_{mb} (Mix Bulk Sp. Gr.)		2.286		% Pass 0.075-mm Sieve	5.1
				G_{mm} (Mix Max. Theor. Sp. Gr.)	2.457

%AV	7.0	%VMA	16.3
% G_{mm}	93.0	%VFA	57.2
		D/AC	1.21

Summary of Mix Design Information
Mix Type: 12.5-mm (ID I-80)

Sieves	SI,mm	%Pass
US	Units	Combnd
1	25	100.0
3/4	19	100.0
1/2	12.5	97.0
3/8	9.5	88.0
#4	4.75	49.0
#8	2.36	30.0
#16	1.18	20.0
#30	0.6	13.0
#50	0.3	8.0
#100	0.15	6.0
#200	0.075	4.2
pan	0	0.0



Percentages of Different Aggregates		
B1	A8	A7
34.0	48.0	18.0

Aggregate Nominal Max Size	12.5 mm
Binder Grade	PG 76-22

$N_{des.}$	125	$N_{initial}$	9	N_{max}	205
G_b (Binder Specific Gravity)		1.022		P_b (% Binder Content)	5.3
G_{sb} (Agg. Bulk Sp. Gr.)		2.654		P_{ba} (absorbed as % mass of agg)	0.6
G_{se} (Aggr. Effective Sp. Gr.)		2.694		P_{be} (effective as % of total mix)	4.8
G_{mb} (Mix Bulk Sp. Gr.)		2.315		% Pass 0.075-mm Sieve	4.2
				G_{mm} (Mix Max. Theor. Sp. Gr.)	2.479

%AV	6.6	%VMA	17.4
% G_{mm}	93.4	%VFA	62.0
		D/AC	0.88

APPENDIX B

GRAPHS PRESENTING FATIGUE TEST RESULTS

I80-60

The code given below describes the various events shown in the plots on the pages that follow:

Temperature:

No. 1	T_0	@ 1.4 million cycles	Indicates out of control. Data after this point is invalid.
No. 2	T_i	@ 1.9 million cycles	Indicates in control. Data after this point is valid.
No. 3	T_0	@ 4.0 million cycles	Indicates out of control. Data after this point is invalid.
No. 4	T_i	@ 4.5 million cycles	Indicates in control. Data after this point is valid.
No. 5	T_0	@ 9.9 million cycles	Indicates out of control. Data after this point is invalid.
No. 6	T_i	@ 11.9 million cycles	Indicates in control. Data after this point is valid.

Attempt to Apply Protocol:

No. 7	A_2	@ 1.89 million cycles	Second attempt at running test, Start Stage I.
No. 8	A_2	@ 4.51 million cycles	Third attempt at running test, Start Stage I.

Start Stage:

No. 9	S_{II}	@ 0.85 million cycles	Start of Stage II (First Attempt)
No. 10	S_{II}	@ 2.67 million cycles	Start of Stage II (Second Attempt)
No. 11	S_{II}	@ 5.18 million cycles	Start of Stage II (Third Attempt)
No. 12	S_{III}	@ 7.83 million cycles	Start of Stage III (Third Attempt)

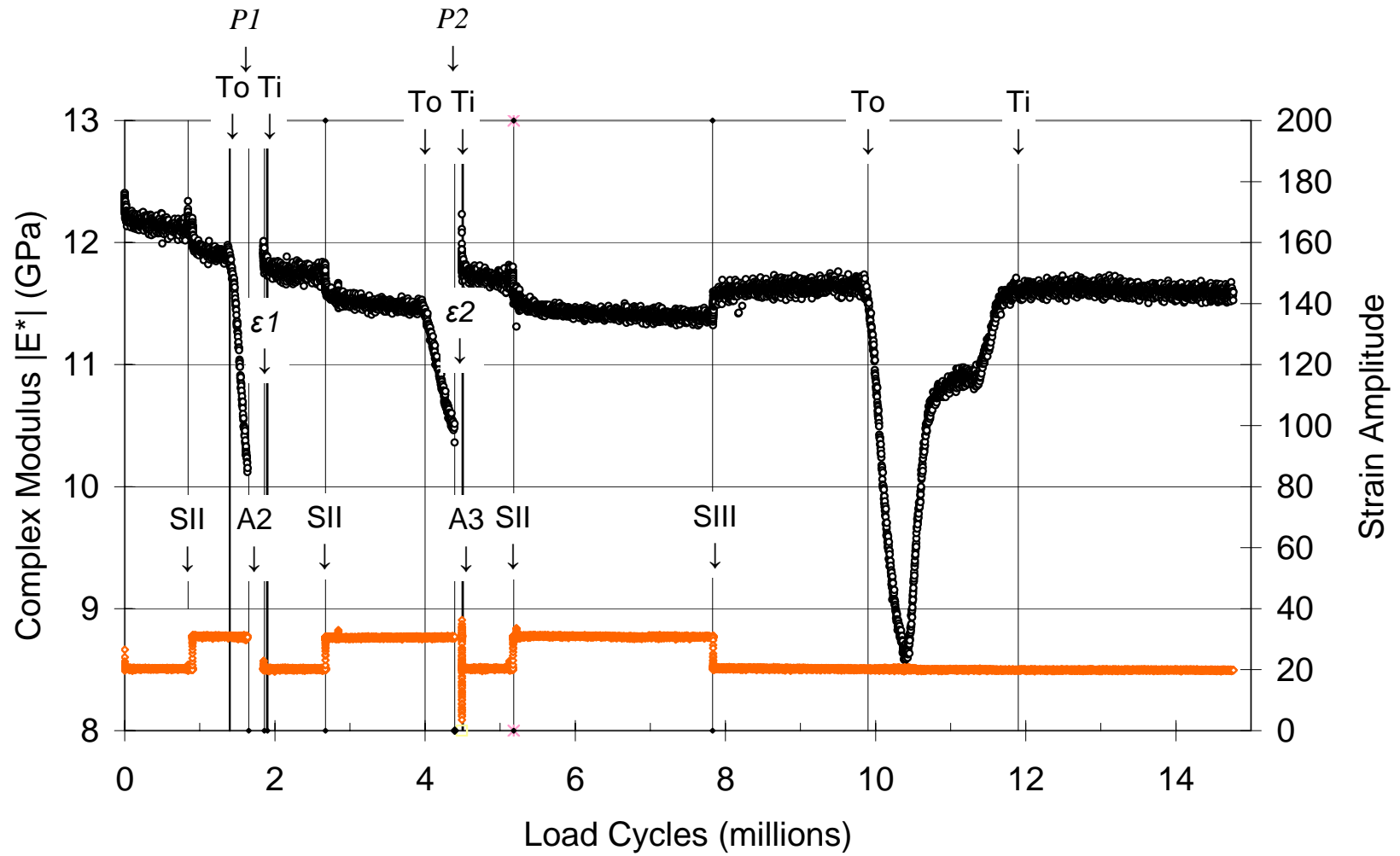
Strain Baseline Adjusted:

No. 13	ϵ_1	@ 1.86 million cycles	Strain baseline adjusted.
No. 14	ϵ_2	@ 4.49 million cycles	Strain baseline adjusted.

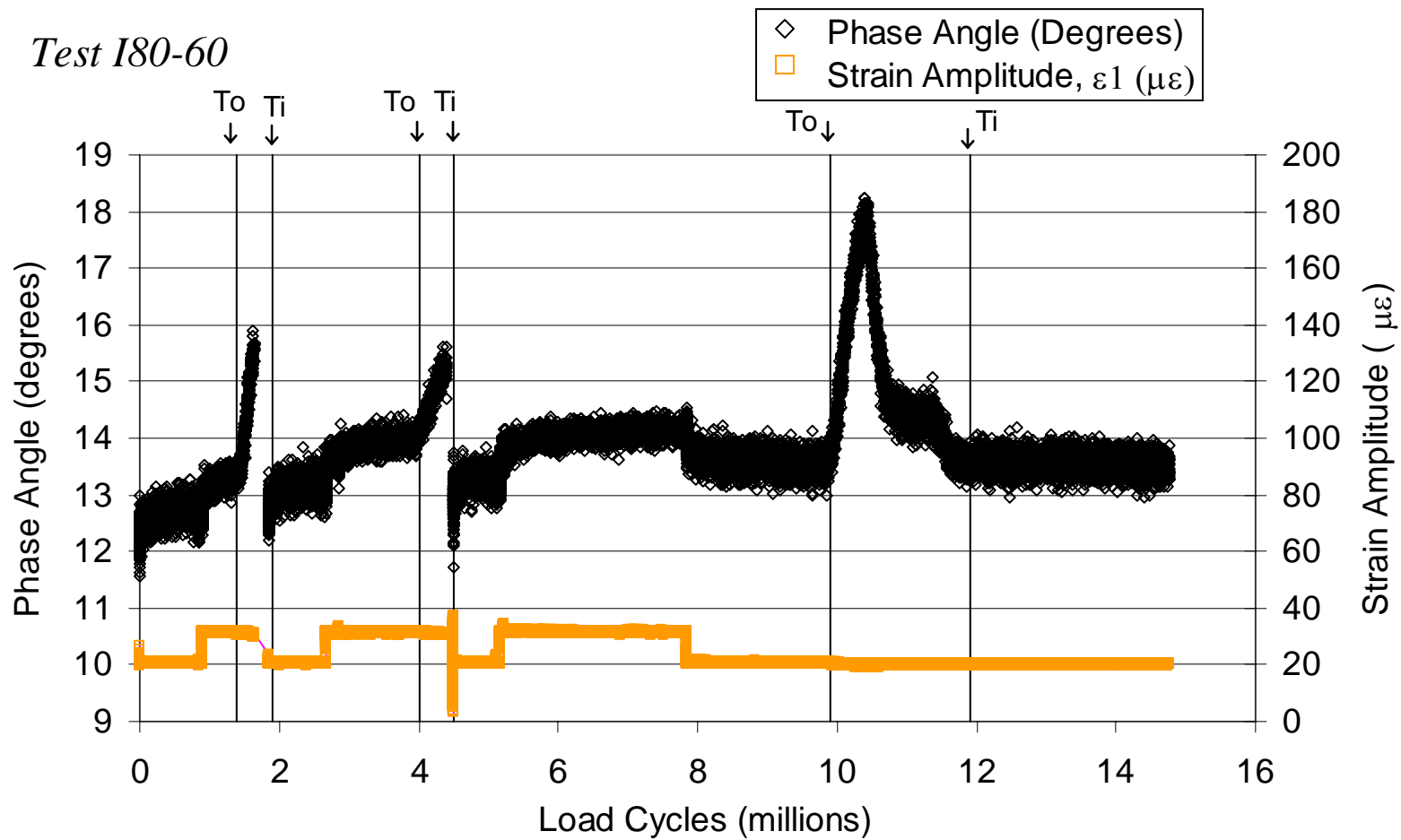
Equipment Issues:

No. 15	P_1	@ 1.65 million cycles	Strain baseline adjusted.
No. 16	P_2	@ 4.40 million cycles	Strain baseline adjusted.

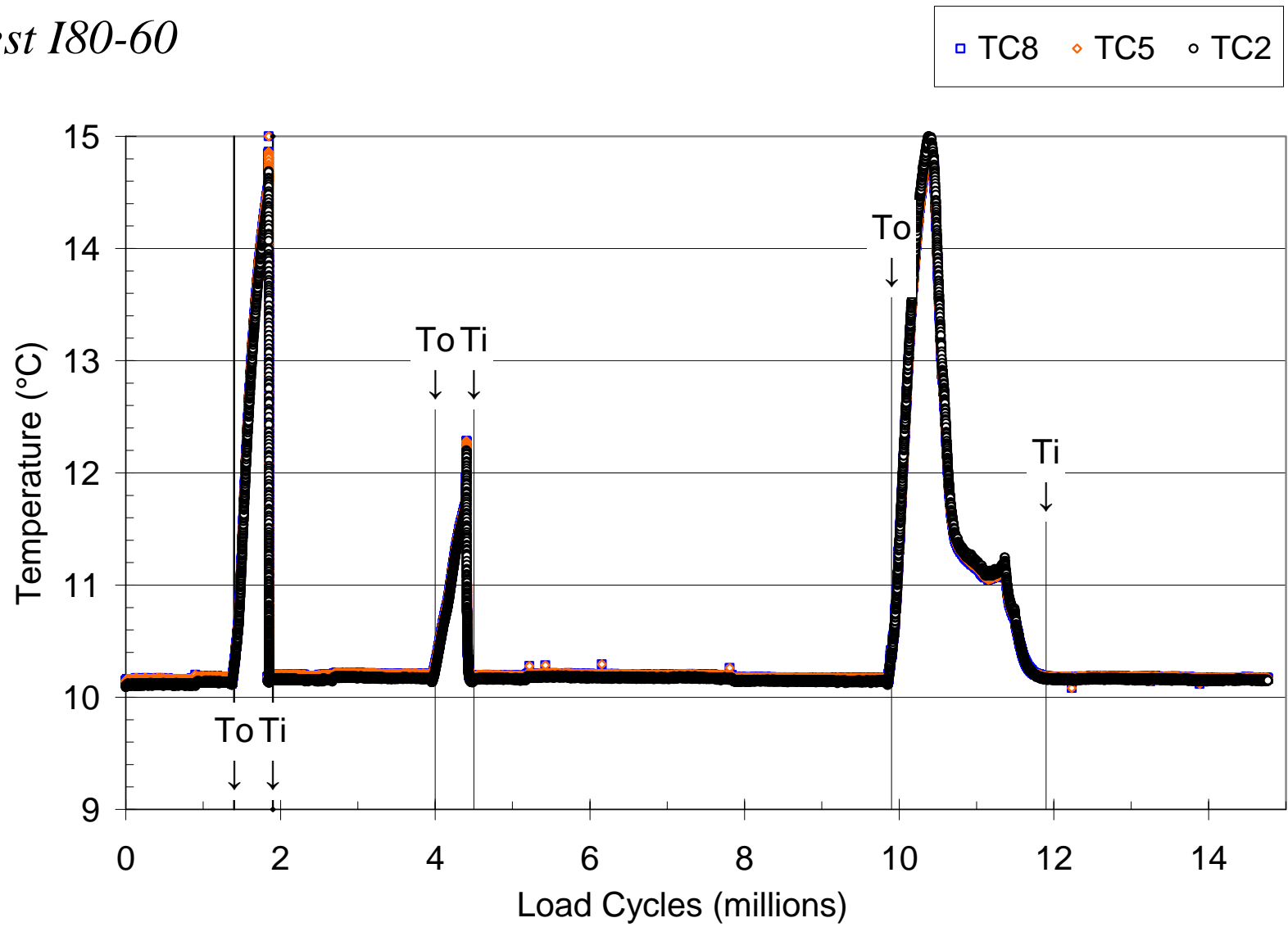
Test I80-60



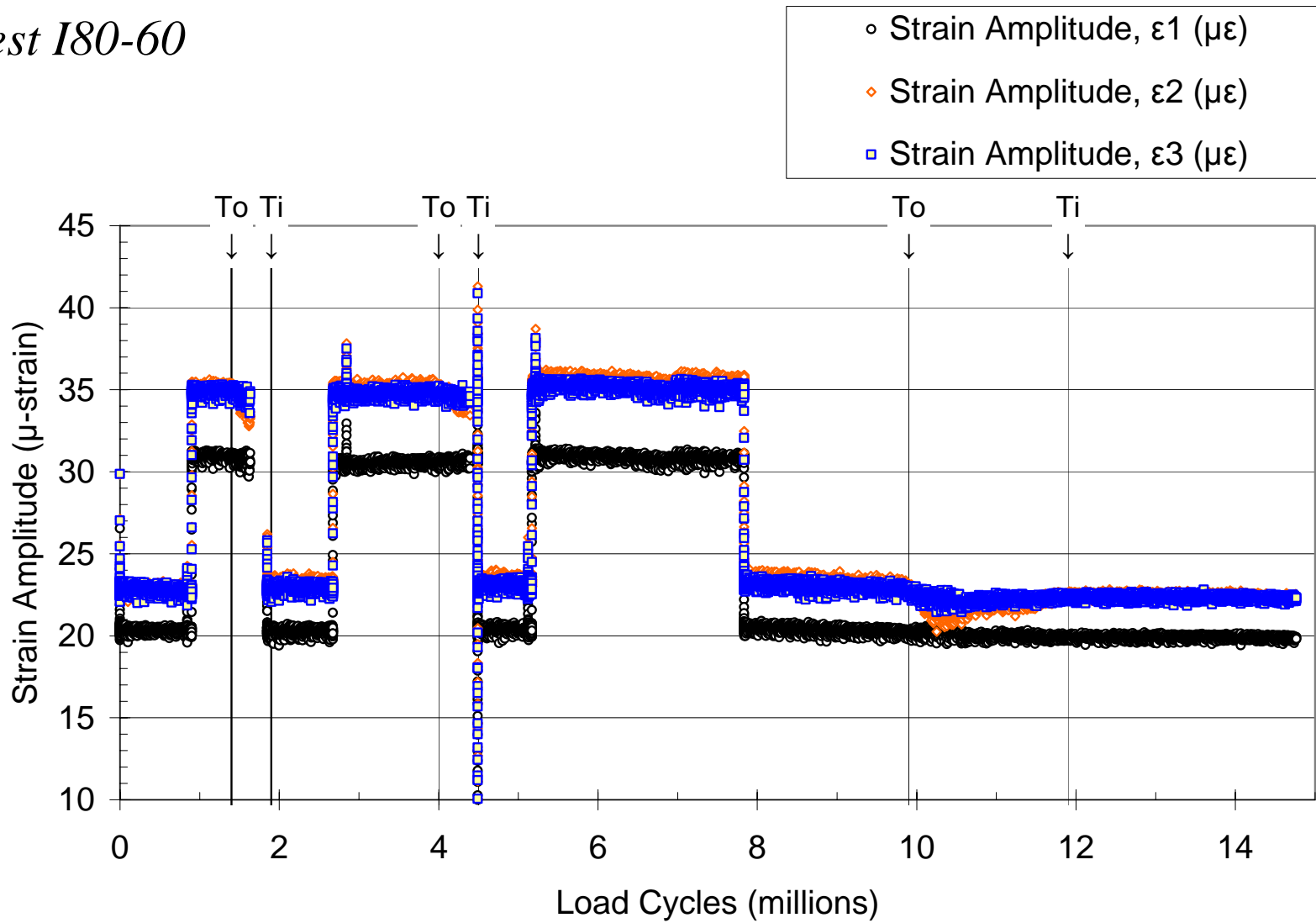
Test I80-60



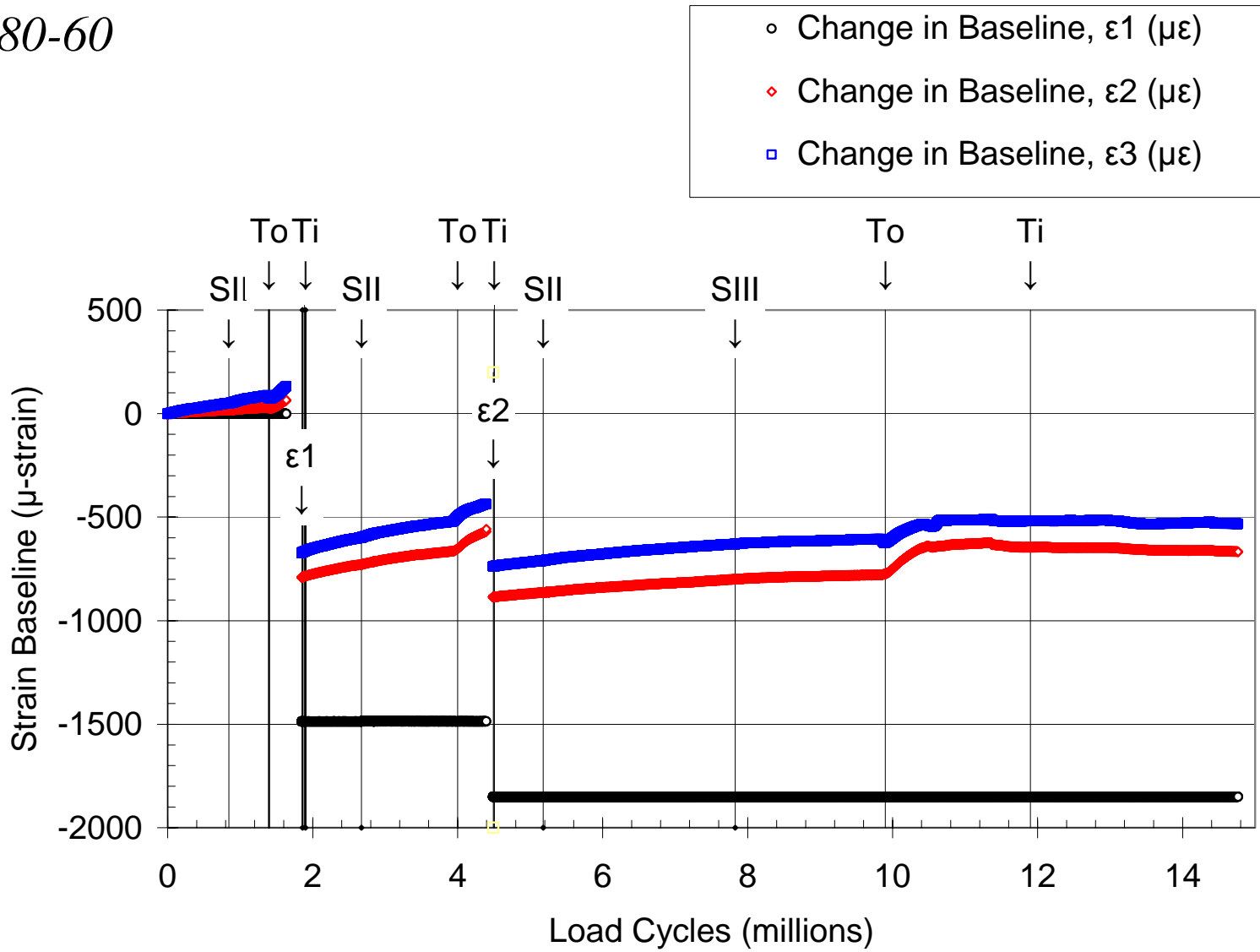
Test I80-60



Test I80-60



Test I80-60



M21673

The code given below describes the various events shown in the plots on the pages that follow:

Start Stage:

No. 1	S _{II}	@ 2.63 million cycles	Stage II started.
No. 2	S _{III}	@ 7.97 million cycles	Stage III started.

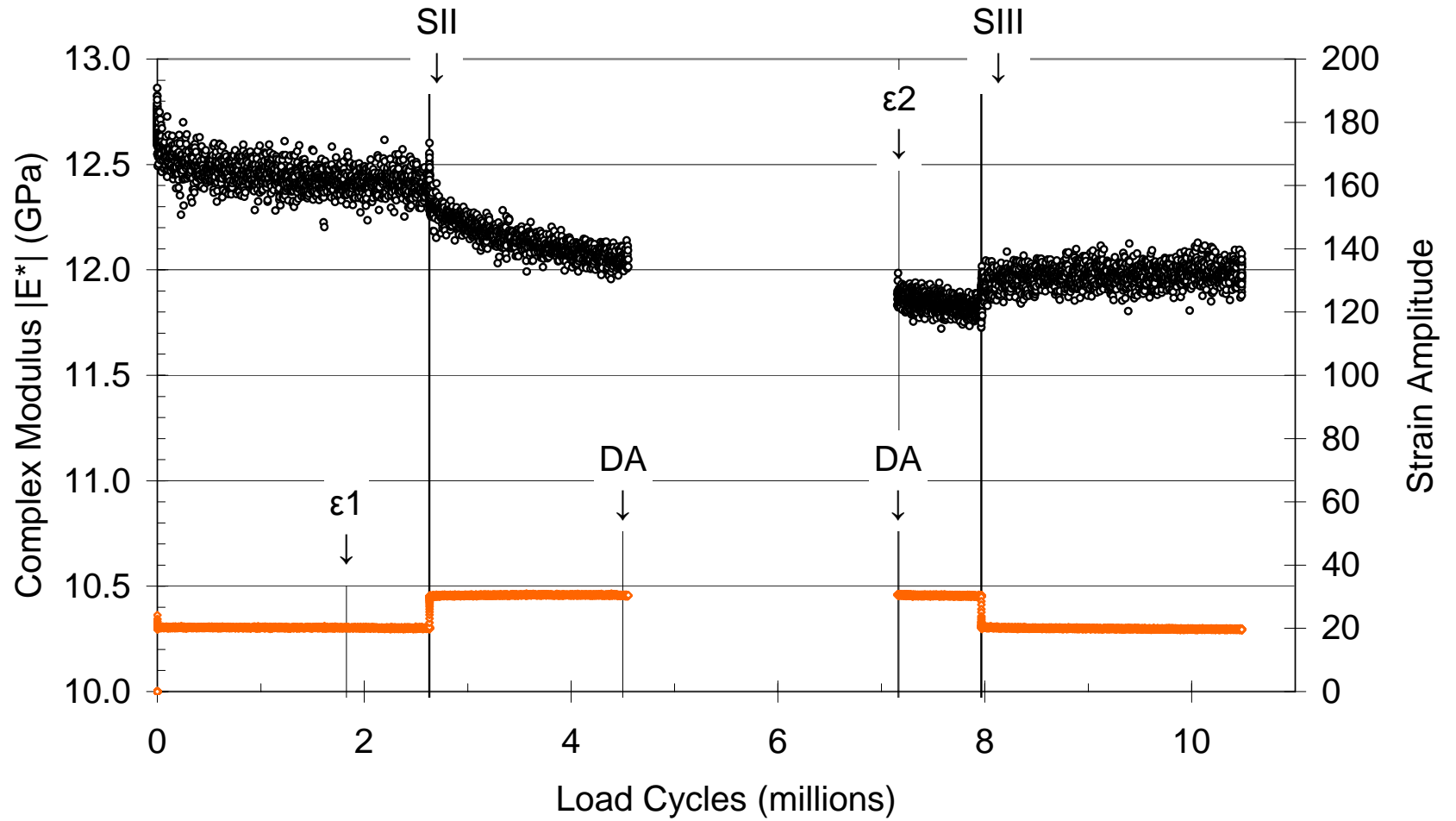
Equipment Issues:

No. 3	DA1	@ 4.50 million cycles	Data acquisition lost, test continued.
No. 4	DA2	@ 7.16 million cycles	Data acquisition regained.

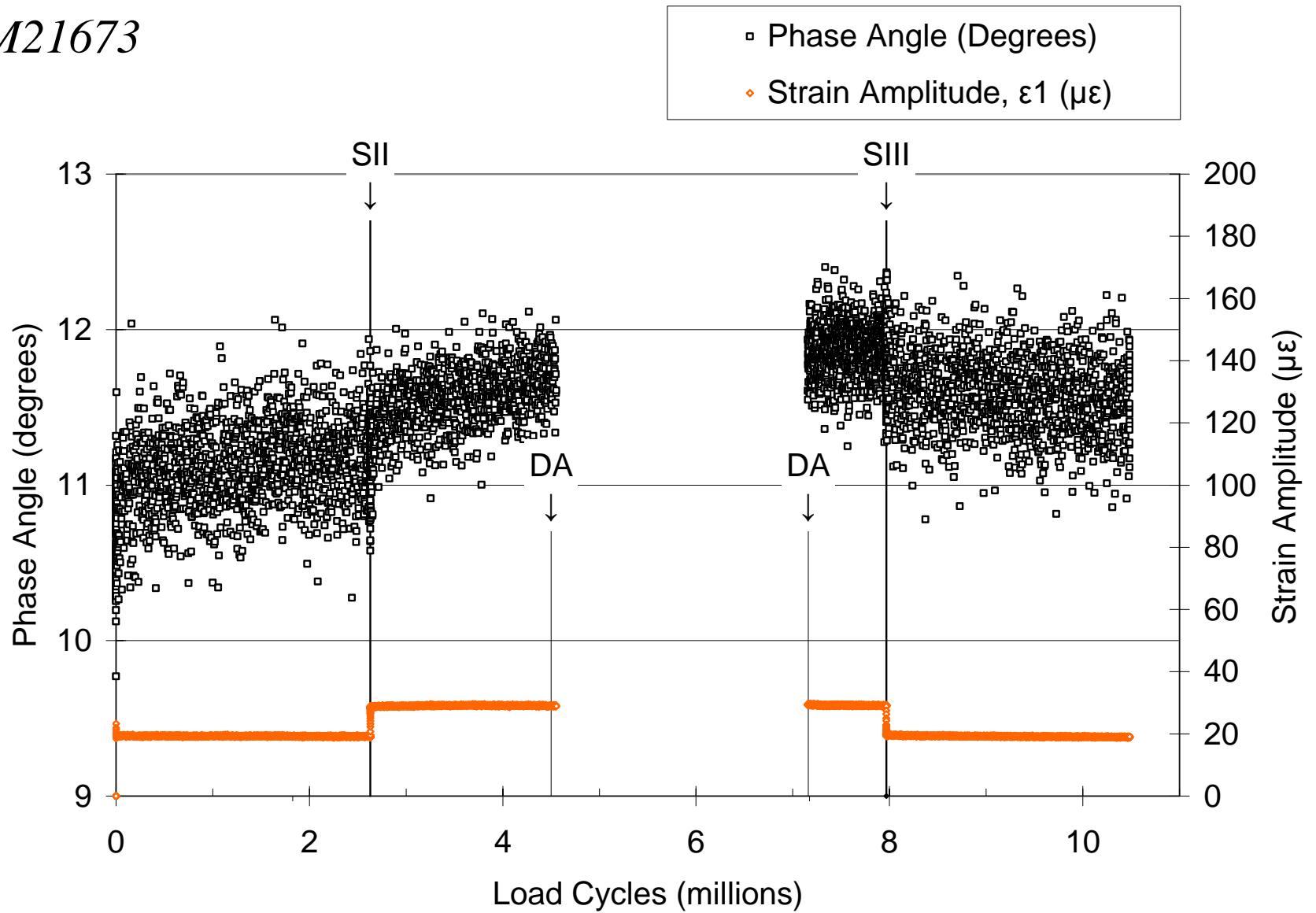
Strain Baseline Adjusted:

No. 5	ε_1	@ 1.83 million cycles	Strain baseline adjusted.
No. 6	ε_2	@ 7.17 million cycles	Strain baseline adjusted.

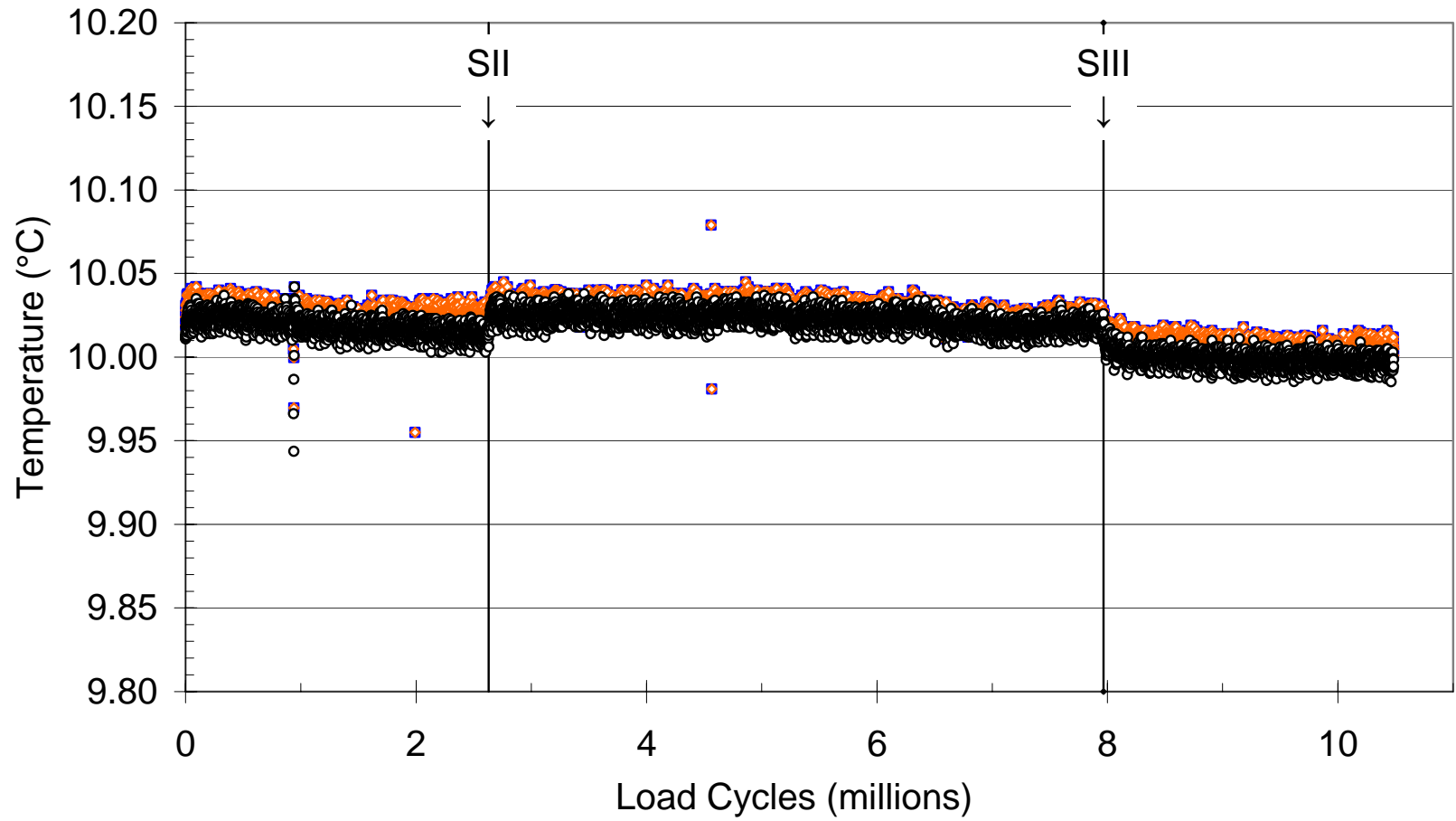
M21673



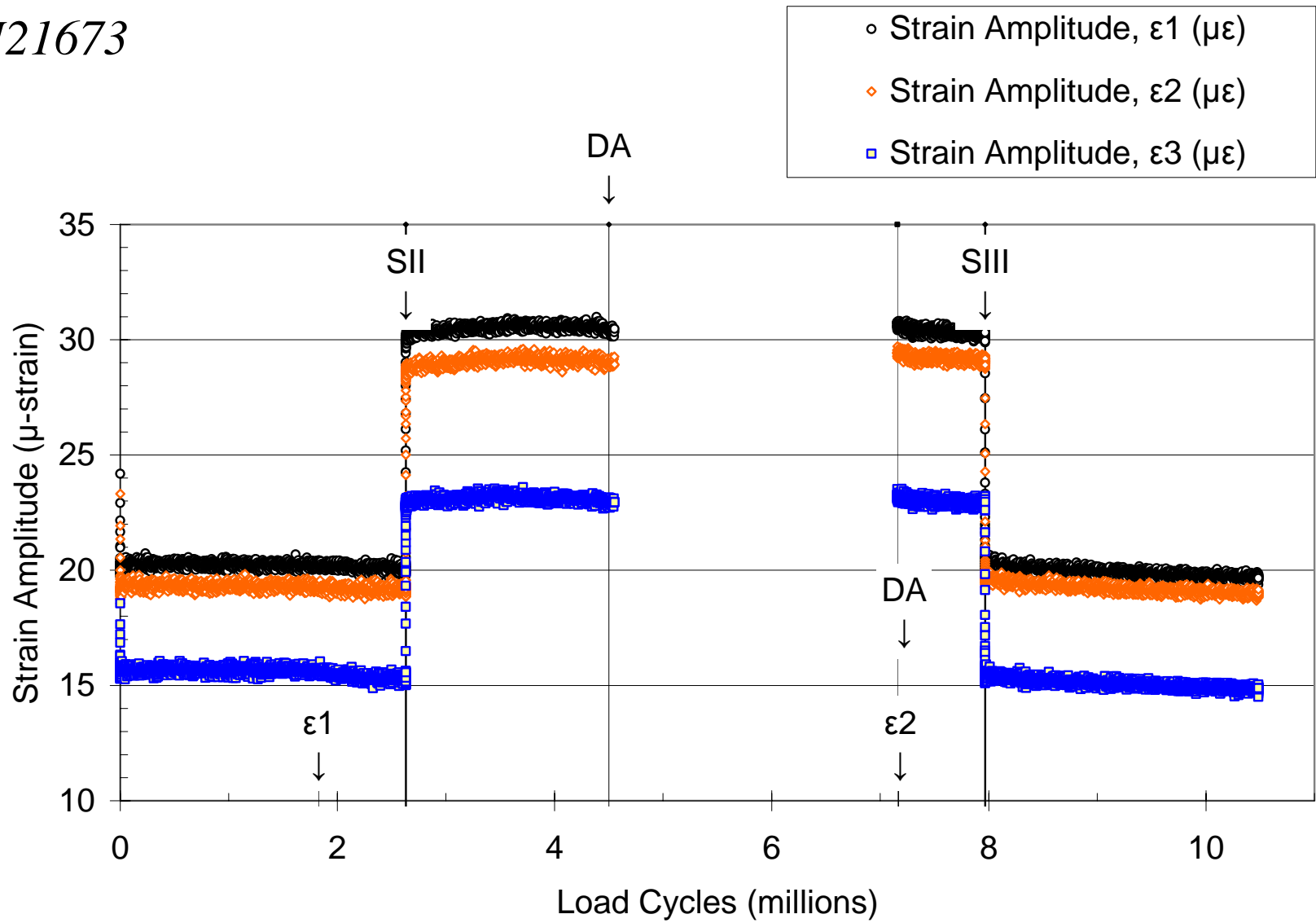
M21673



M21673

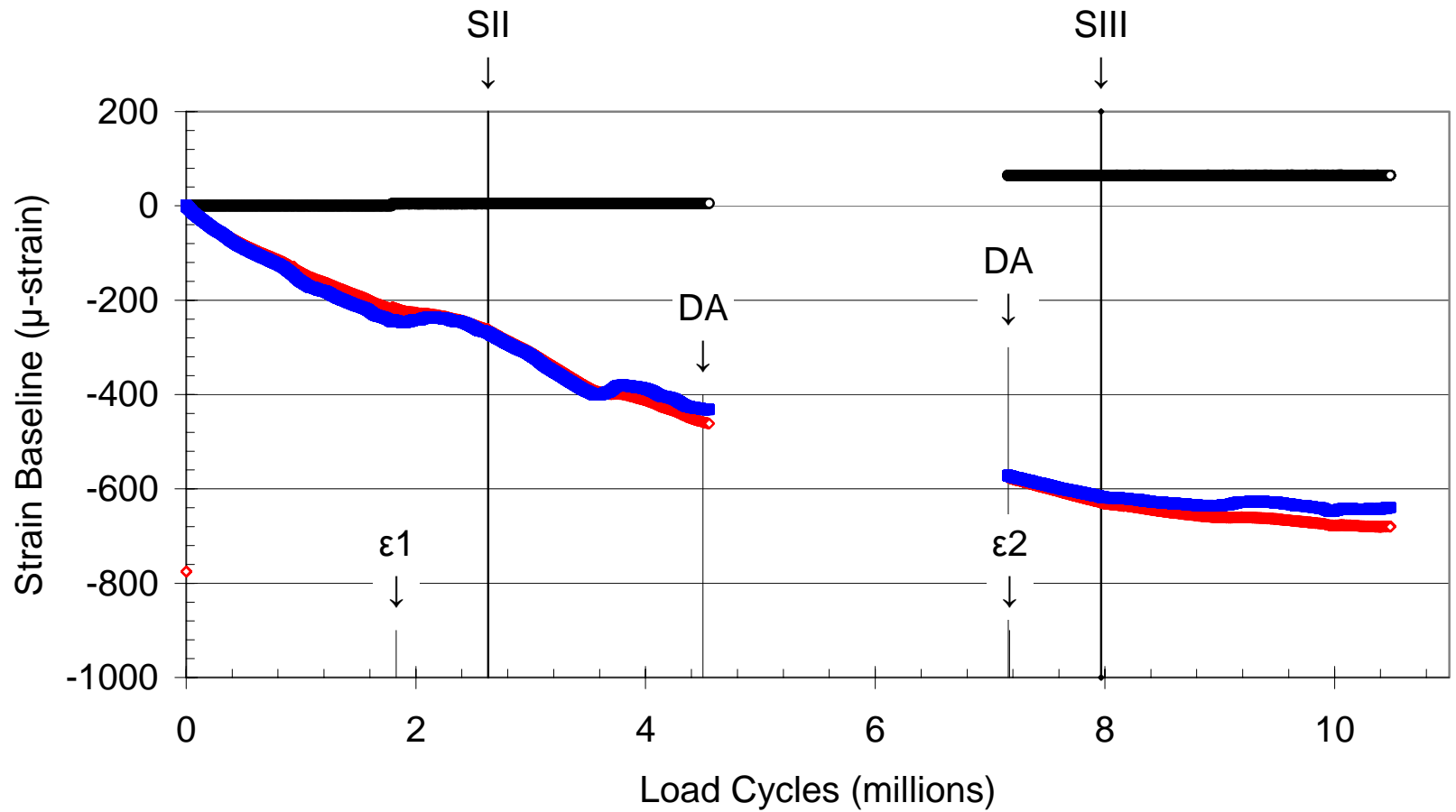


M21673



M21673

- Change in Baseline, ϵ_1 ($\mu\epsilon$)
- ◇ Change in Baseline, ϵ_2 ($\mu\epsilon$)
- Change in Baseline, ϵ_3 ($\mu\epsilon$)



M21676

The code given below describes the various events shown in the plots on the pages that follow:

Temperature:

- | | | | |
|-------|-------|-----------------------|--|
| No. 1 | T_0 | @ 4.52 million cycles | Indicates out of control. Data after this point is invalid |
| No. 2 | T_i | @ 4.52 million cycles | Indicates in control. Data after this point is valid |

Attempt to Apply Protocol:

- | | | | |
|-------|-------|-----------------------|--|
| No. 3 | A_2 | @ 4.52 million cycles | Second attempt at running test, Start Stage I. |
|-------|-------|-----------------------|--|

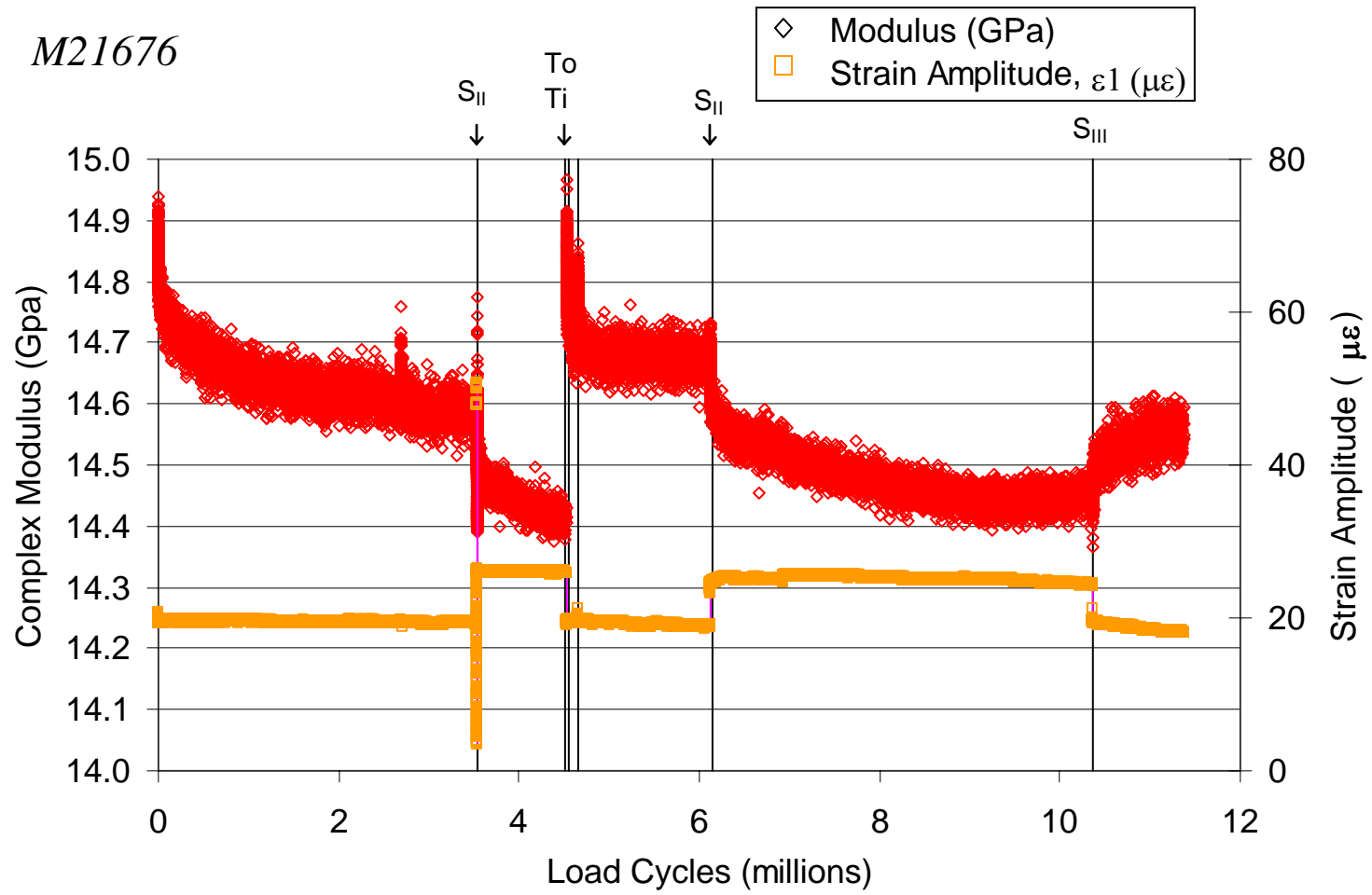
Start Stage:

- | | | | |
|-------|-----------|------------------------|--------------------------------------|
| No. 4 | S_{II} | @ 3.54 million cycles | Start of Stage II (First Attempt). |
| No. 5 | S_{II} | @ 6.14 million cycles | Start of Stage II (Second Attempt). |
| No. 6 | S_{III} | @ 10.37 million cycles | Start of Stage III (Second Attempt). |

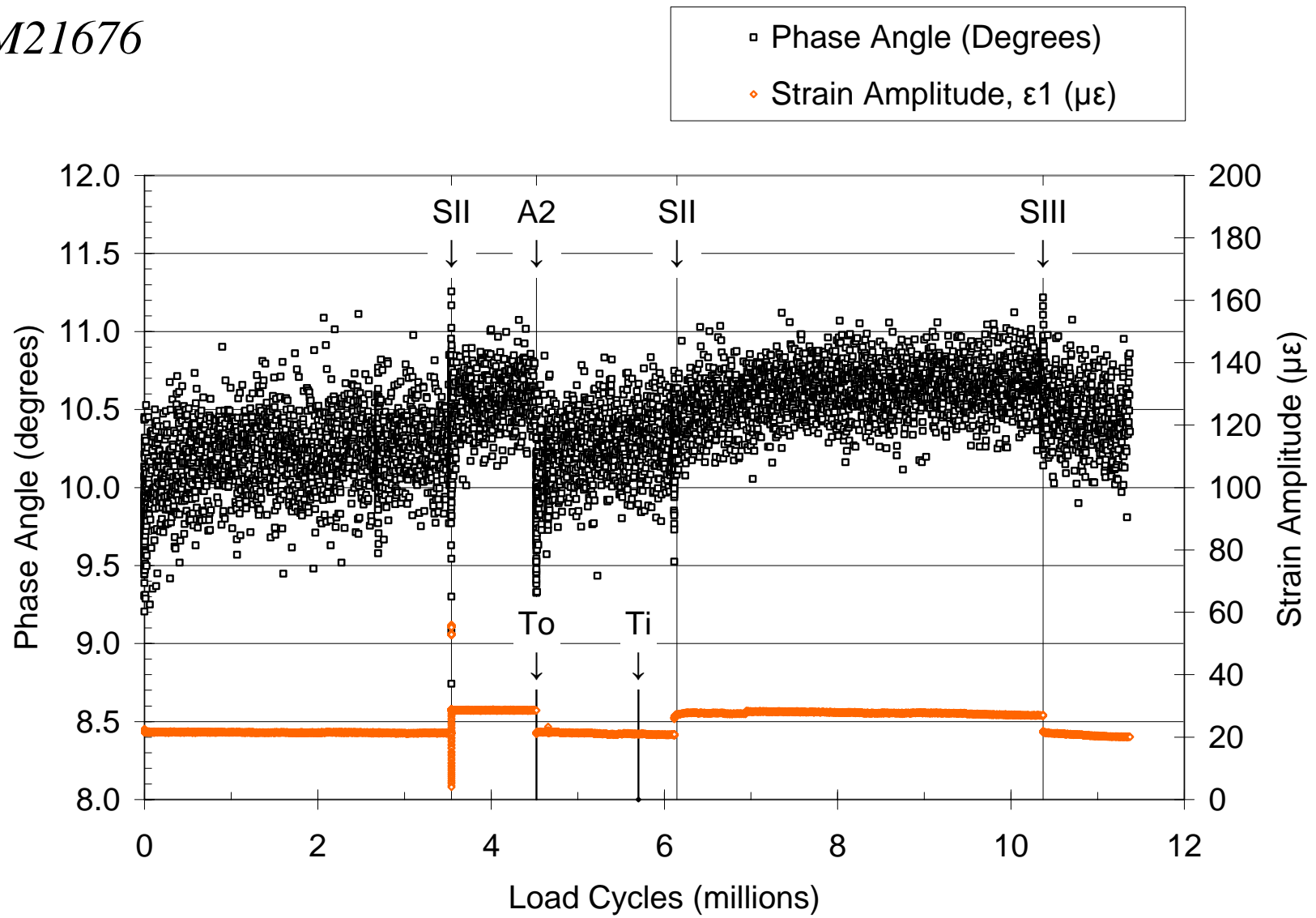
Strain Baseline Adjusted:

- | | | | |
|-------|--------------|-----------------------|---------------------------|
| No. 7 | ϵ_1 | @ 4.55 million cycles | Strain baseline adjusted. |
| No. 8 | ϵ_2 | @ 4.66 million cycles | Strain baseline adjusted. |
| No. 9 | ϵ_3 | @ 5.87 million cycles | Strain baseline adjusted. |

M21676

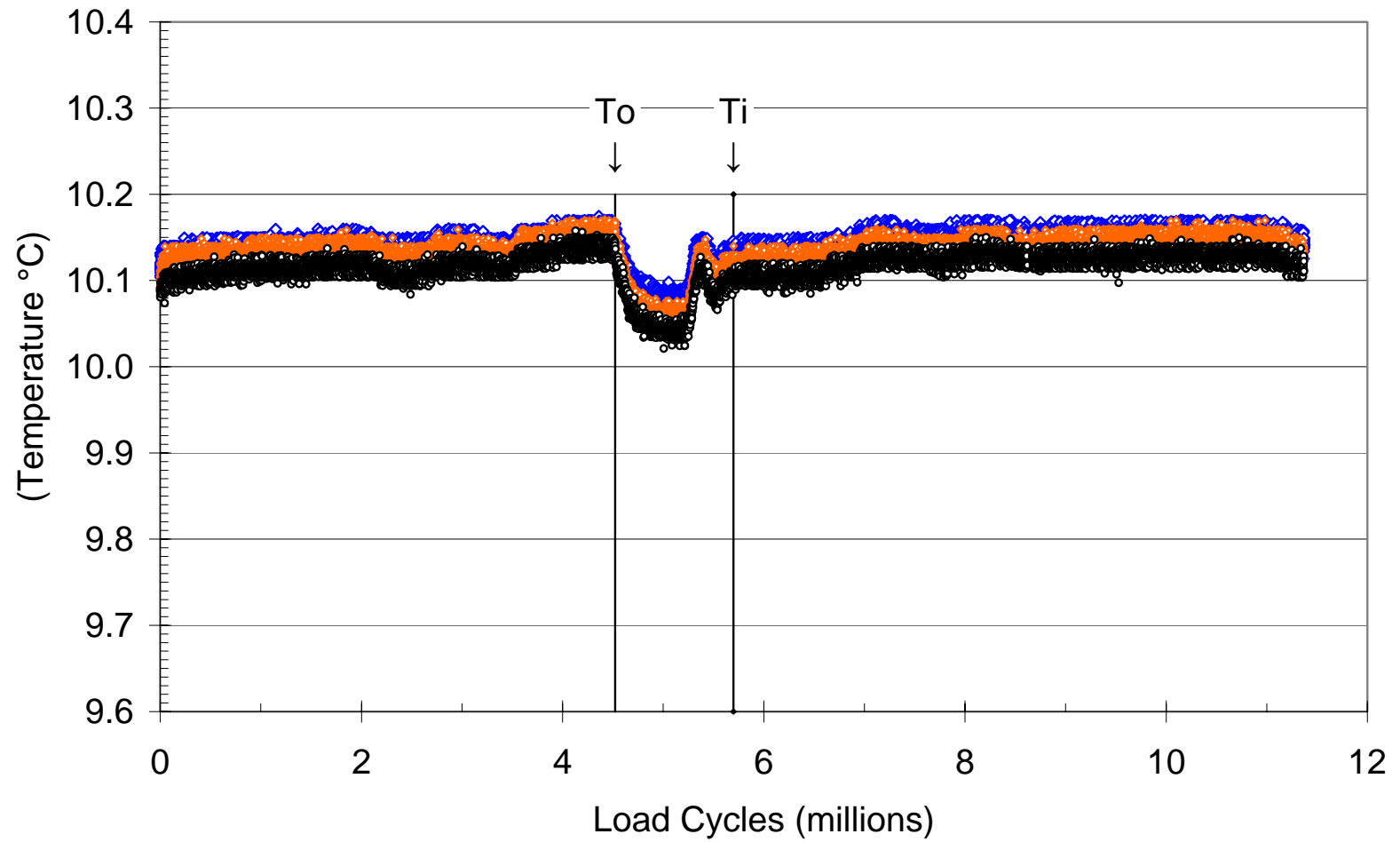


M21676

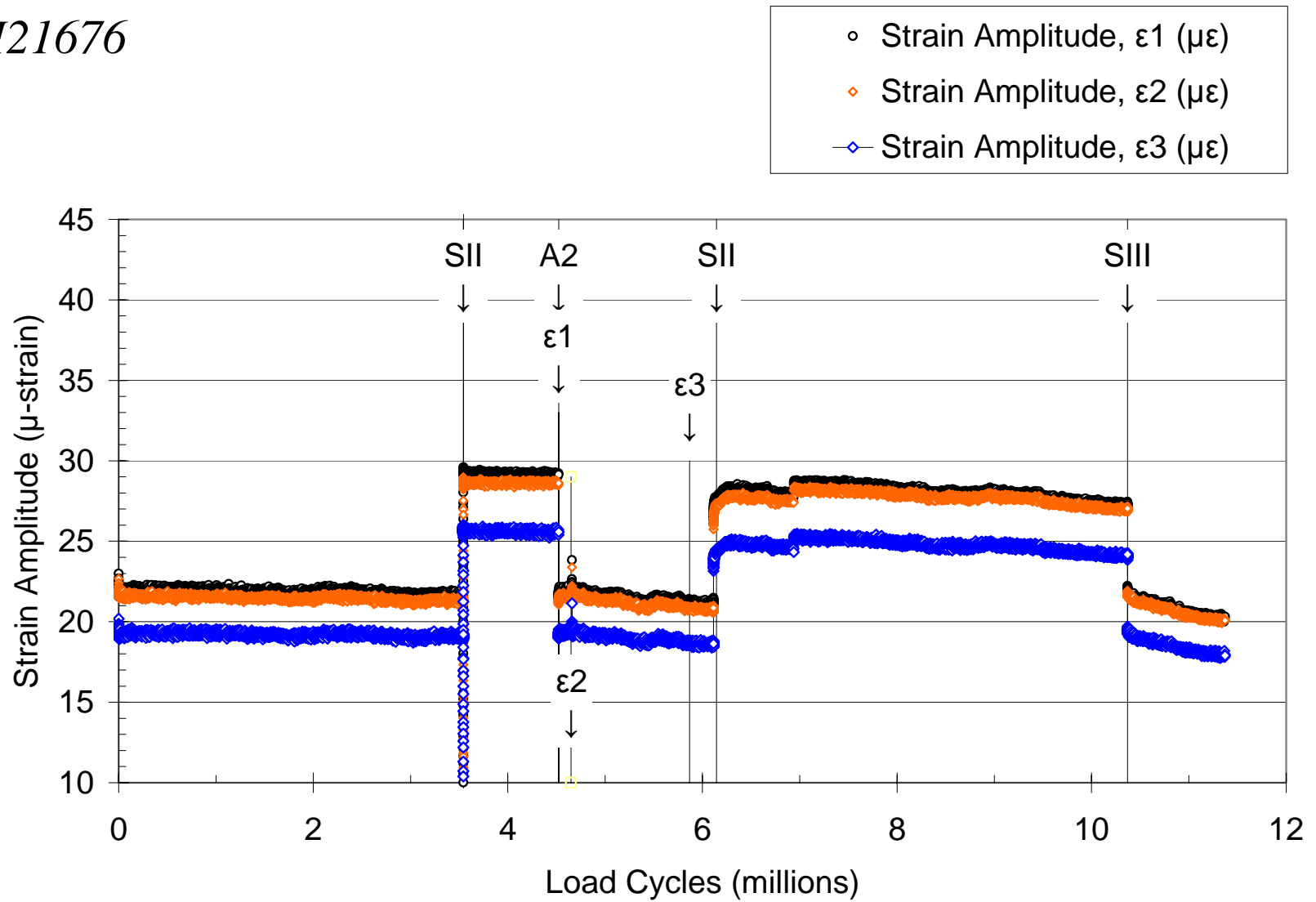


M21676

◇ TC8 ◇ TC5 ◦ TC2

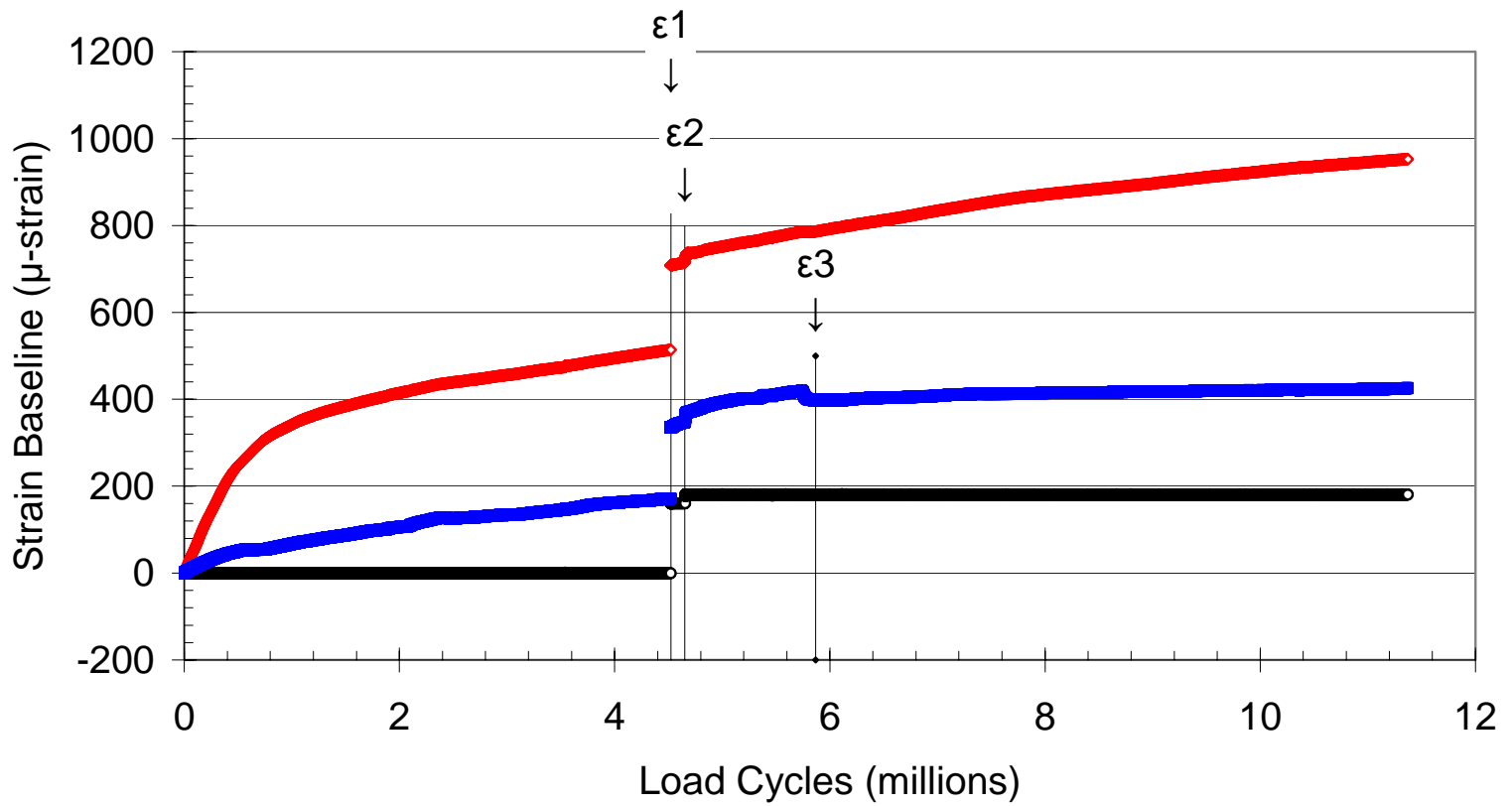


M21676



M21676

- Change in Baseline, ϵ_1 ($\mu\epsilon$)
- ◇ Change in Baseline, ϵ_2 ($\mu\epsilon$)
- Change in Baseline, ϵ_3 ($\mu\epsilon$)



M32986

The code given below describes the various events shown in the plots on the pages that follow:

Attempt to Apply Protocol:

No. 1	A_2	@ 3.23 million cycles	Second attempt to apply protocol.
-------	-------	-----------------------	-----------------------------------

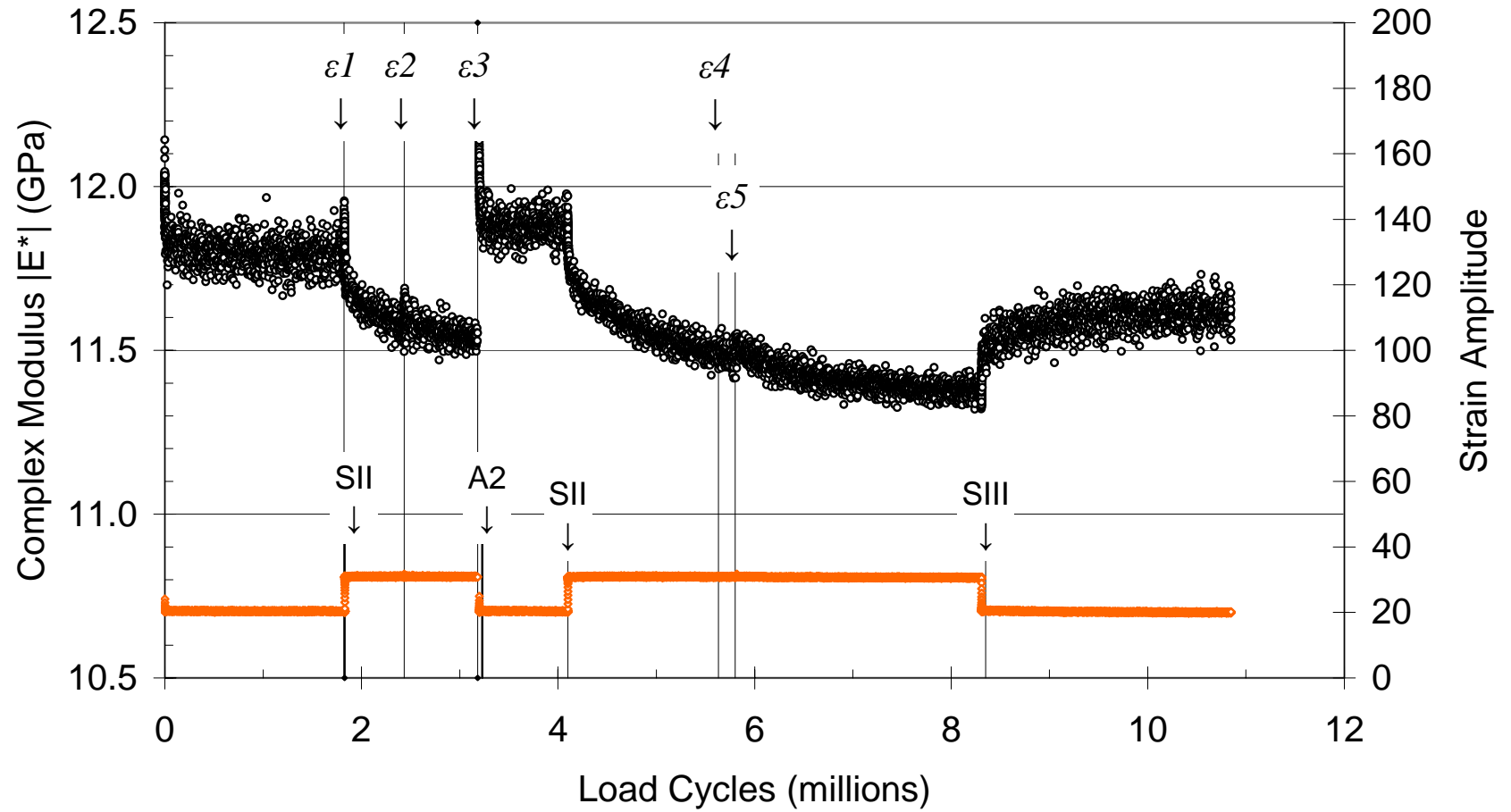
Start Stage:

No. 2	S_{II}	@ 1.83 million cycles	Start of Stage II in 1 st attempt.
No. 3	S_{II}	@ 4.10 million cycles	Start of Stage II for 2 nd attempt.
No. 4	S_{III}	@ 8.35 million cycles	Start of Stage III for 2 nd attempt.

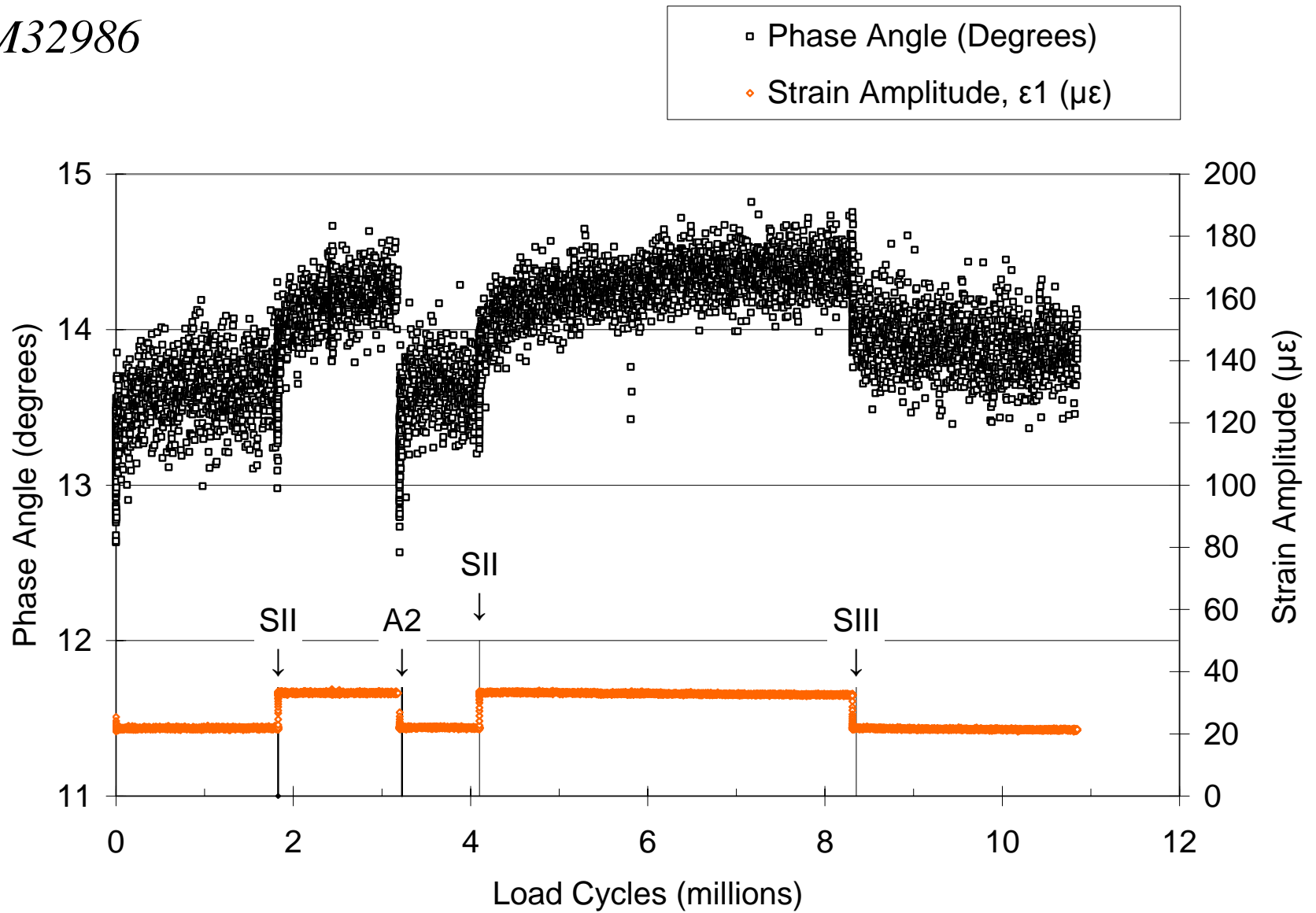
Strain Baseline Adjusted:

No. 5	ε_1	@ 1.82 million cycles	Strain baseline adjusted.
No. 6	ε_2	@ 2.44 million cycles	Strain baseline adjusted.
No. 7	ε_3	@ 3.18 million cycles	Strain baseline adjusted.
No. 8	ε_4	@ 5.63 million cycles	Strain baseline adjusted.
No. 9	ε_5	@ 5.80 million cycles	Strain baseline adjusted.

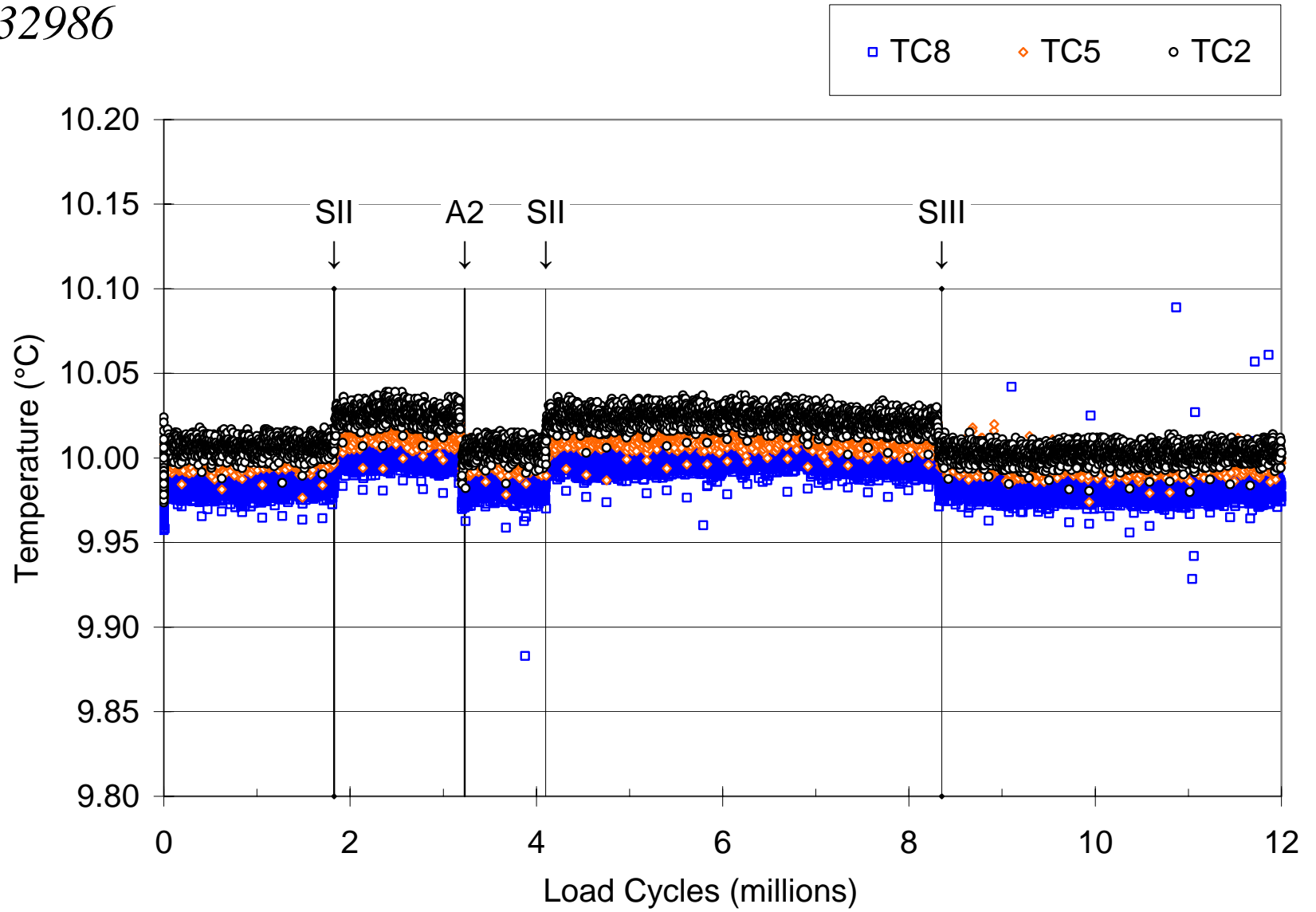
M32986



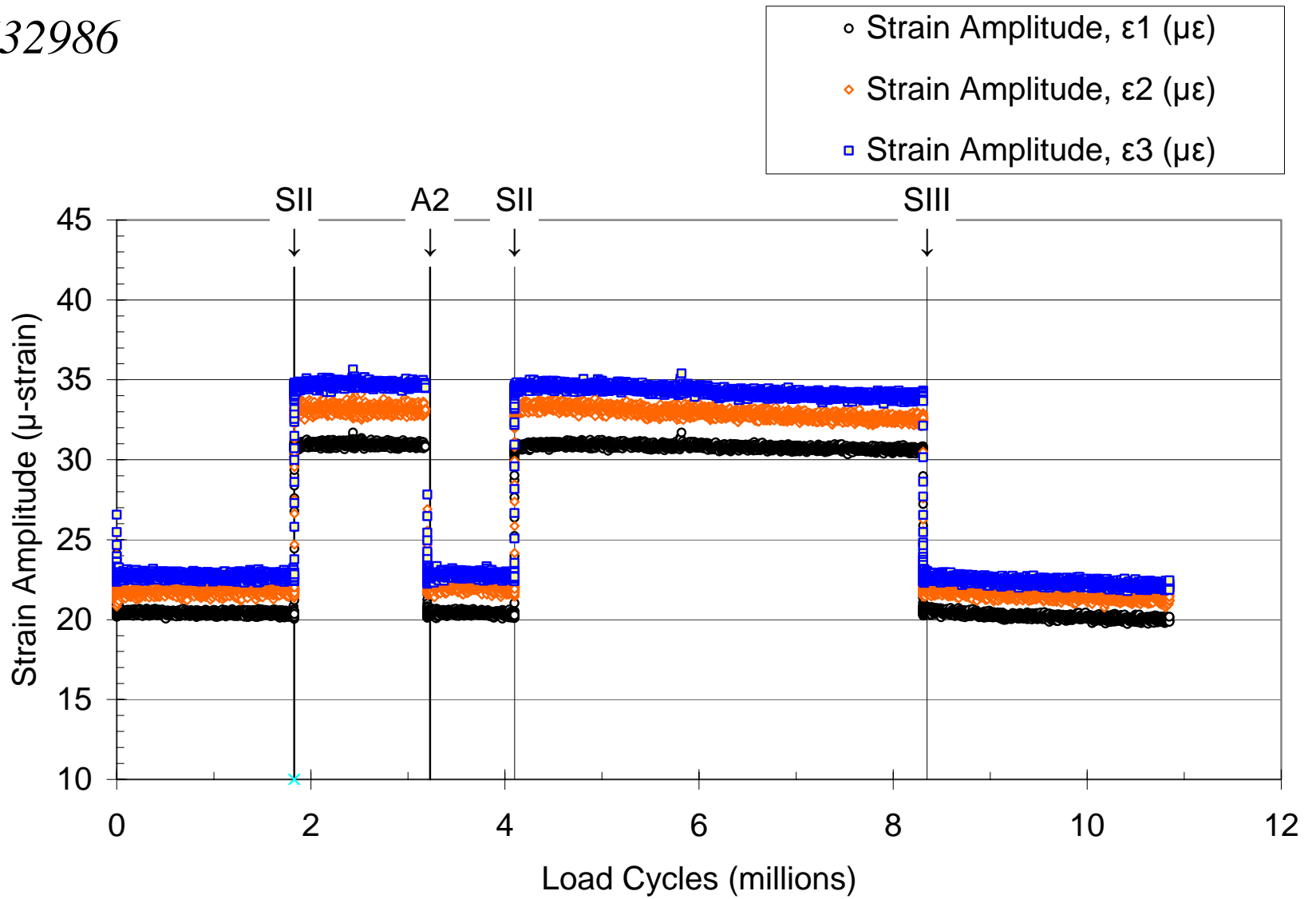
M32986



M32986



M32986



M32986

- Change in Baseline, ϵ_1 ($\mu\epsilon$)
- ◇ Change in Baseline, ϵ_2 ($\mu\epsilon$)
- Change in Baseline, ϵ_3 ($\mu\epsilon$)

